Journal of Materials Chemistry B

ROYAL SOCIETY OF CHEMISTRY

REVIEW

View Article Online
View Journal | View Issue

Cite this: J. Mater. Chem. B, 2022, 10, 6059

An update on biomaterials as microneedle matrixes for biomedical applications

Xiao Peng Zhang,†[ab] Yu Ting He,†[ab] Wen Xuan Li,[ab] Bo Zhi Chen,*[ab] Can Yang Zhang,*[c] Yong Cui*[d] and Xin Dong Guo *[ab]

Received 26th April 2022,
Accepted 16th June 2022

DOI: 10.1039/d2tb00905f

rsc.li/materials-b

Microneedles (MNs) have been developed for various applications such as drug delivery, cosmetics, diagnosis, and biosensing. To meet the requirements of MNs used in these areas, numerous materials have been used for the fabrication of MNs. However, MNs will be exposed to skin tissues after piercing the stratum corneum barrier. Thus, it is necessary to ensure that the matrix materials of MNs have the characteristics of low toxicity, good biocompatibility, biodegradability, and sufficient mechanical properties for clinical application. In this review, the matrix materials currently used for preparing MNs are summarized and reviewed in terms of these factors. In addition, MN products used on the market and their applications are summarized in the end. This work may provide some basic information to researchers in the selection of MN matrix materials and in developing new materials.

1. Introduction

The transdermal drug delivery route is more easily accepted by patients because it is painless, non-invasive, and convenient for patients compared with hypodermic injections.[1–3] However, due to the strong barrier of the stratum corneum layer, the ideal matrix materials for the preparation of transdermal drug delivery patches should meet the properties of low molecular mass (less than 600 Da), moderate lipophilicity (log p1–3) and low melting point.[4–7] At present, only about 20 drugs that meet these requirements have been approved by the Food and Drug Administration (FDA) for the preparation of transdermal drug delivery patches.[8] Based on these issues, MNs have been developed for transdermal drug delivery to overcome the barrier of the stratum corneum to promote the delivery of drugs.

MNs are painless micro-size devices that can breach the stratum corneum hence producing recoverable tiny channels on the skin without stimulating pain-sensitive nerves. In fact, as early as the 1970s, MNs were envisioned for drug delivery,[9] and during the late 1990s, Henry *et al.* first published their study on the use of silicon MNs. The experimental results indicated that the insertion of MNs into the skin was capable of dramatically increasing the transport of molecules across the skin, which further confirmed the feasibility of MNs for transdermal administration.[10,11] Since then, MNs have been constantly growing for various purposes such as drug delivery,[12] cosmetics,[13] diagnosis and biosensing.[14–16] Among them, the typical applications of MNs are the delivery of drugs, especially for the macromolecule drugs such as peptides, proteins and antibodies, since these biomacromolecules are easily digested or metabolized in the gastrointestinal tract by the oral route.[17,18]

Naturally, to meet the requirements of MNs used in different areas, the matrix materials of MNs have also been developed from silicon materials to a variety of materials such as glass, metals, ceramics, oligosaccharides, and polymers. Jae-Min Song *et al.*[19] used a traditional stainless-steel material to prepare metal MNs for H5N1 influenza virus-like particle delivery, which is expected to be used for self-vaccination against a virus with pandemic potential. To achieve the smart release of insulin, Wang *et al.*[20] designed novel charge-switchable polymeric complex MNs for glucose-responsive insulin delivery in mice and pigs. Based on the dissolving properties of carboxymethyl cellulose, Lee *et al.*[21] fabricated a kind of lidocaine-loaded MN array for rapid and painless local anesthesia. These studies have shown the great potential of MNs for clinical application as minimally invasive and painless devices. However, MN arrays will be exposed to the viable skin tissue after piercing the stratum corneum barrier. Thus, it is necessary to ensure that the matrix materials of MNs have the characteristics of

[a] State Key Laboratory of Organic–Inorganic Composites, Beijing University of Chemical Technology, Beijing, 10029, China. E-mail: xdguo@buct.edu.cn, chenbz@mail.buct.edu.cn
[b] Beijing Laboratory of Biomedical Materials, College of Materials Science and Engineering, Beijing University of Chemical Technology, Beijing, 100029, P. R. China
[c] Biopharmaceutical and Health Engineering Division, Tsinghua Shenzhen International Graduate School, Shenzhen, 518055, China. E-mail: zhang.cy@sz.tsinghua.edu.cn
[d] Department of Dermatology, China–Japan Friendship Hospital, East Street Cherry Park, Chaoyang District, Beijing, 100029, P. R. China. E-mail: wuhucuiyong@vip.163.com
† Both authors contributed equally to this work.

low toxicity, good biocompatibility, biodegradability, and good mechanical properties for clinical application. In this work, the matrix materials currently used for preparing MNs are summarized in terms of these factors, which gives an outlook of the future development of MNs. In addition, MN products used in the market and their applications are summarized in the end. Hoping this work could provide some basic information to researchers in the selection of MN matrix materials and in the development of new materials.

2. Matrix materials and properties

Generally, MNs can be categorized as solid, hollow, coated, dissolving and hydrogel-forming MNs according to their drug delivery strategies (Fig. 1). Solid MNs are mainly prepared using some materials with good mechanical properties to enhance skin permeability.[22–24] The removal of solid MNs from the skin produces temporary tiny holes to enhance the penetration of drugs. Hollow MNs were typically used for delivering liquid formulations and the drug flow rate and flow rate can be controlled by adjusting the amount of inlet pressure.[25–27] Coated MNs are usually prepared by coating water-soluble formulations on solid MNs.[28] After insertion of the coated MNs, the drug coatings are dissolved into the skin within a certain time, and then the MNs are removed. Differently, dissolving MNs are usually fabricated by water-soluble materials, and the drug formulations can be encapsulated in the matrix materials of dissolving MNs and released after insertion.[29,30] Hydrogel-forming MNs swell to release drugs or extract bodily fluids after contact with skin interstitial fluid (ISF).[31]

The matrix materials for the fabrication of these types of MNs can be roughly divided into silicon, glass, ceramics, metals, oligosaccharides and polymers. The percentage of publications on different matrix materials of MNs in the last 5 years as shown in Fig. 2. More than half of the published literature on MNs is on polymer and oligosaccharide MNs, and this has been increasing over the last five years. In this section, the mechanical properties of these matrix materials and their safety such as toxicity and biocompatibility will be summarized and discussed.

2.1. Silicon

With the development of a high-precision microelectronic technology, silicon is considered an excellent mechanical material that can be used to design a variety of desirable shapes (Fig. 3A).[5,32] Based on these advantages, silicon was selected as a matrix material to prepare the first MNs (150 μm-tall) for transdermal drug delivery.[11] Subsequently, silicon has been widely used to fabricate solid and hollow MN arrays with various geometric parameters for drug delivery.[9,33] Until now, research on silicon MNs still accounts for a proportion (Fig. 2).

Although silicon has the characteristics of high fracture strength and toughness, there is still a risk that the sharp tips of silicon MNs may fracture under the skin during application due to the brittle nature of silicon.[34] Besides, silicon is not an FDA-approved biomaterial, and its biocompatibility has not been well established up to now. Thus, these fractured silicon fragments remaining under the skin may cause undesirable immunogenic consequences or be transported *via* blood vessels to the heart and cause arterial blockage.[35] Several methods have been proposed to solve the fracture and biocompatibility issues of silicon MNs, such as coating some higher strength and biocompatibility metal layers such as gold or silver (Fig. 3B and C)[27,36] or designing the shape of MNs according to strength theories such as maximum linear strain theory and Tresca yield criterion.[37] Thus, the length of silicon MNs usually is shorter than that of others. Narayanan and colleagues fabricated solid silicon MNs with an average height of 158 μm, base width of 110.5 μm, tip angle of 19.4° and tip diameter of 0.40 μm by optimizing silicon etching technique factors.[38] These silicon MNs were proven to be strong enough to penetrate the skin without any breakage, and the microchannels formed by silicon MNs on the skin surface can improve the drug delivery rate (Fig. 3D).[39] However, silicon MNs are still very expensive because the preparation of silicon MNs requires extensive processing and clean room facilities. At the same time, the researchers focused more on microneedles prepared from other materials, given the problems of bacterial infections that can occur when the skin is left open for long periods of time after the solid microneedles have been prepped to form microchannels in the skin.[40]

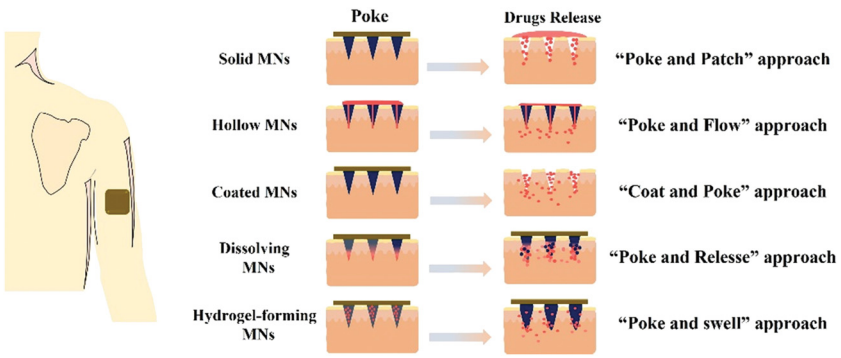

Fig. 1 Schematic diagram of different MN administrations.

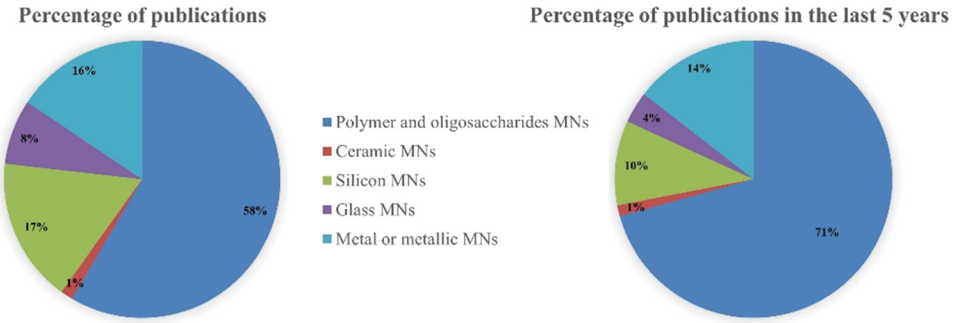

Fig. 2 Percentage of publications on different matrix materials of MNs, based on Web of Science (https://apps.webofknowledge.com/). Keywords used were 'polymer microneedle', 'oligosaccharide microneedle', 'silicon microneedle', 'glass microneedle', 'ceramic microneedle', 'metal microneedle' and 'metallic microneedle'. Reviews are not included. Search date: 3 April 2022.

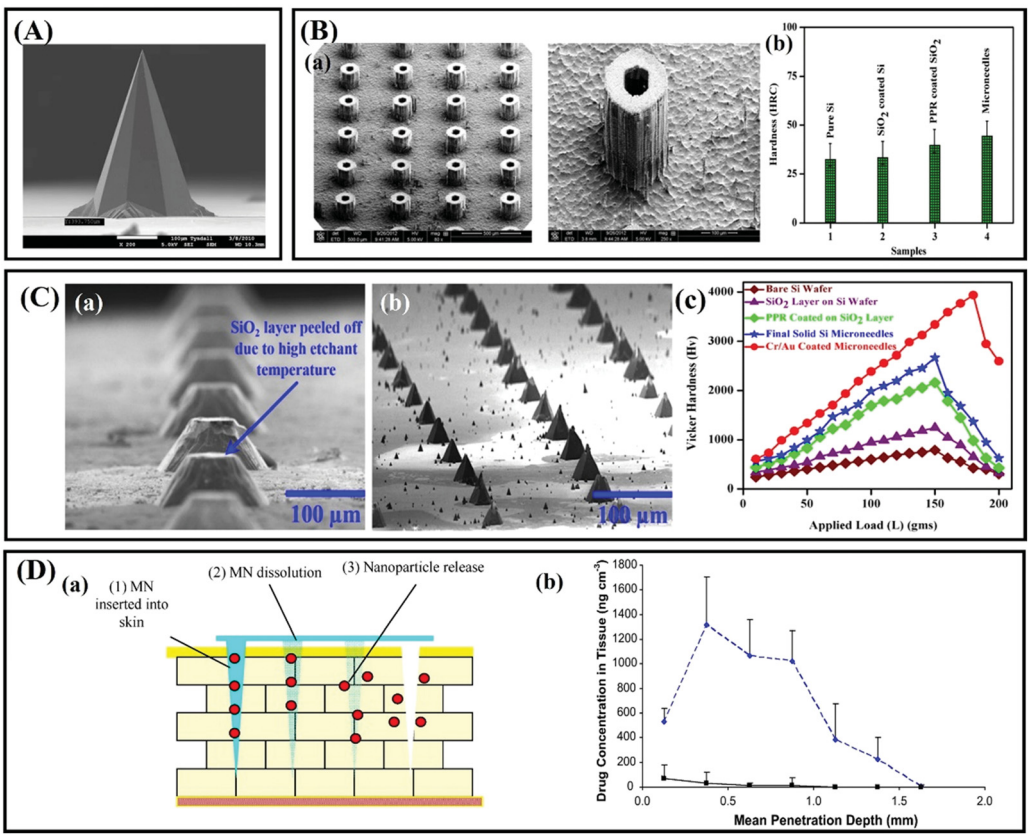

Fig. 3 (A) Solid silicon MNs (height: ~400 µm. Adapted with permission from ref. 34. Copyright 2014 Springer Nature. (B) (a) SEM image of hollow silicon MNs. (b) Vickers hardness test measured and compared for solid Si MNs. Adapted with permission from ref. 27. Copyright 2014 Elsevier. (C) (a) Single row of MNs with the SiO_2 layer peeled off. (b) Final high aspect ratio of solid Si MNs. (c) Measured and compared-load *versus* Vickers hardness (Hv) values for all samples. Adapted with permission from ref. 36. Copyright 2018 Springer Nature. (D) (a) Schematic representation of the steps involved in Nile Red release from the polymeric MN system. (b) The concentration of Nile Red in excised neonatal porcine skin following the application of PMVE/MA MNs containing Nile Red-loaded nanoparticles and control patches containing Nile red nanoparticles. Adapted with permission from ref. 39. Copyright 2010 Elsevier.

2.2. Glass

Glass is a kind of material which is cheap, physiologically and chemically inert, easily sterilized, and easily fabricated in various geometries.[41,42] The excellent transparent property of glass permits easy visualization of fluid flow. Prausnitz *et al.* fabricated a kind of hollow glass MN using borosilicate glass based on the micropipette puller technology to extract dermal ISF for glucose monitoring (Fig. 4A).[43] The results showed that the glass MNs could each withstand more than 1 kg of force before breaking and no evidence of adverse skin reactions was observed.[43] Their group also designed 0.9 mm-long, 30° beveled hollow borosilicate glass MNs to test the hypothesis of

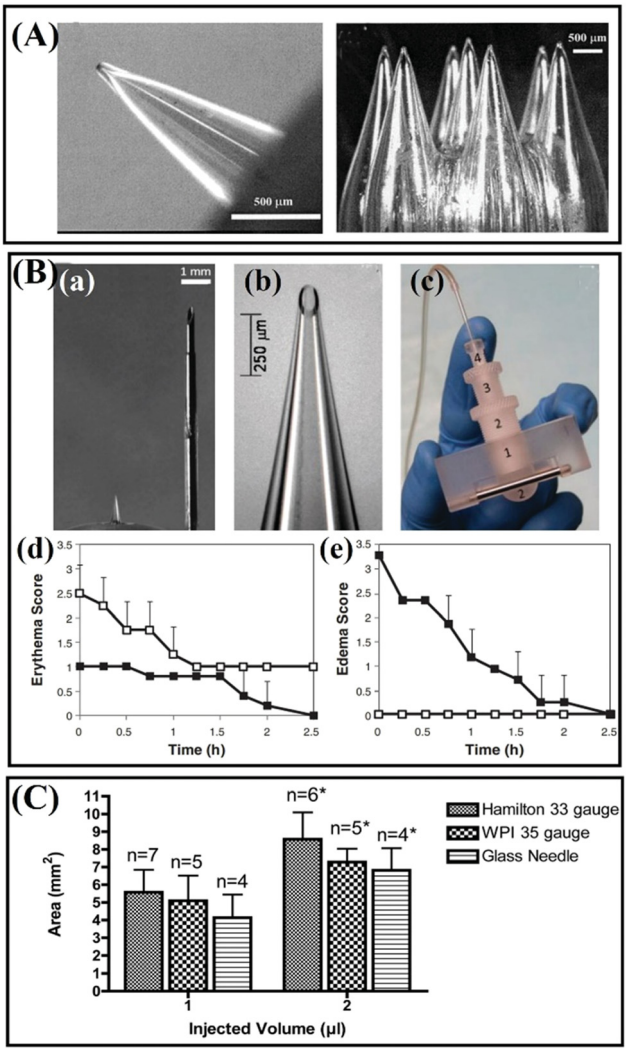

Fig. 4 (A) Images of hollow glass MNs fabricated to pierce the skin to extract ISF for glucose monitoring (the glass MNs were fabricated using a thermal puller). Adapted with permission from ref. 43. Copyright 2005 Mary Ann Liebert Inc. (B) (a–c) Images of hollow MNs. (d and e) Local skin reaction at the site of insulin administration. (d) Erythema and (e) edema scores for subcutaneous 0.9 mm catheter (open symbols) and intradermal 0.9 mm-long MN (solid symbols) treatment sites using the Dermal Draize scale. Adapted with permission from ref. 25. Copyright 2011 Mary Ann Liebert Inc. (C) Corneal area affected after intrastromal injection of 1 μL or 2 μL India ink using different needle types. *$P < 0.05$ compared with 1 μL injection using the same needle type. Adapted with permission from ref. 45. Copyright 2012 Springer Nature.

intradermal insulin infusion in human subjects.[25] The MNs could be fabricated strong enough to insert into the skin without breakage by controlling the preparation parameters, and intradermal MN injection caused significantly less erythema compared with subcutaneous catheter infusion (Fig. 4B).[25] However, due to the remarkable chemical inertness and low chemical reactivity of glass, it is difficult to prepare glass-based MNs by chemical methods, so currently, glass-based MNs are usually produced by the traditional method of pulling glass rods using an aspirator, which is not very efficient in production. Therefore, the use of glass MNs are only limited to small experimental scales, and the commercial settings have not been achieved.[25,41,44]

Additionally, like silicon MNs, glass MNs also suffer from the brittle problem during application. Matthaei and colleagues used hand-pulled and 25° beveled glass MNs to deliver India ink into the eyes of mice.[45] The results suggested that the glass needle tends to provide the smallest absolute affected area, and the injection using Hamilton 33 G needles and WPI 35 G needles shows a trend to affect the larger absolute staining area (Fig. 4C), but the glass needles may break inside the corneal stroma. However, Experiments have proved that borosilicate glass implants appear to be biocompatible with the cortical surface[45,46] but there is a risk that silica glass may cause granulomas in the skin.[5] For pharmaceutical purposes, borosilicate glass may be better than silica glass.

2.3. Ceramics

Ceramics have been widely used for skeletal repair and reconstruction materials.[47–50] Also, these materials have aroused great interest of researchers in the preparation of MNs due to their outstanding properties such as good strength, excellent chemical resistance, and biocompatibility.[26,51] Importantly, the surface area, porosity and degradation of ceramics can be tailored during the fabrication process, so ceramic-based MNs can be designed for controlled release of drugs.[52–54] Alumina is the commonly used material for ceramic MNs.[55,56] Boks and coworkers fabricated a kind of alumina-based nanoporous ceramic MNs for controlled release of a model vaccine (Fig. 5A).[57] Notably, a study carried out by Bystrova and coworkers showed that the unreasonable drying conditions of the alumina green tape could result in breakage of the MNs during demolding.[51] Studies have suggested that a risk that the role of aluminum release from alumina implants must be considered when alumina implants are used for long term implants, but alumina shows good biocompatibility for short term implants and basically will not cause adverse reactions such as redness, swelling (Fig. 5B).[58,59]

Alumina-based ceramic MNs are usually fabricated using micromolding and sintering. The extremely sinter temperature of ceramic MNs, even as high as 1500 °C, resulted in drugs only can be loaded into the MNs after sintering.[60,61] Therefore, a kind of self-setting ceramics such as gypsum and brushite have been proposed for the fabrication of MNs, because these materials have good resorbability, biocompatibility, and the slurries of these ceramics can be cured at room temperature or under mild condition instead of high temperature sintering.[62,63] Cai and colleagues fabricated a type of self-setting bioceramic MNs using alpha calcium sulphate hemihydrate ($CaSO_4 \cdot 0.5H_2O$, α-CSH), β-Tricalcium phosphate ($Ca_3(PO_4)_2$), and monocalcium phosphate monohydrate ($Ca(H_2PO_4)_2 \cdot H_2O$) for transdermal drug delivery.[63] The experiments suggested that the porosity and resorbability of the self-setting MNs can be used to regulate the release behavior, and these MNs have good mechanical strength to penetrate the skin without breakages (Fig. 5C).[63] Vallhov and coworkers also prepared the MNs using $CaSO_4 \cdot 0.5H_2O$ and the experiment proved that approximately 90% of

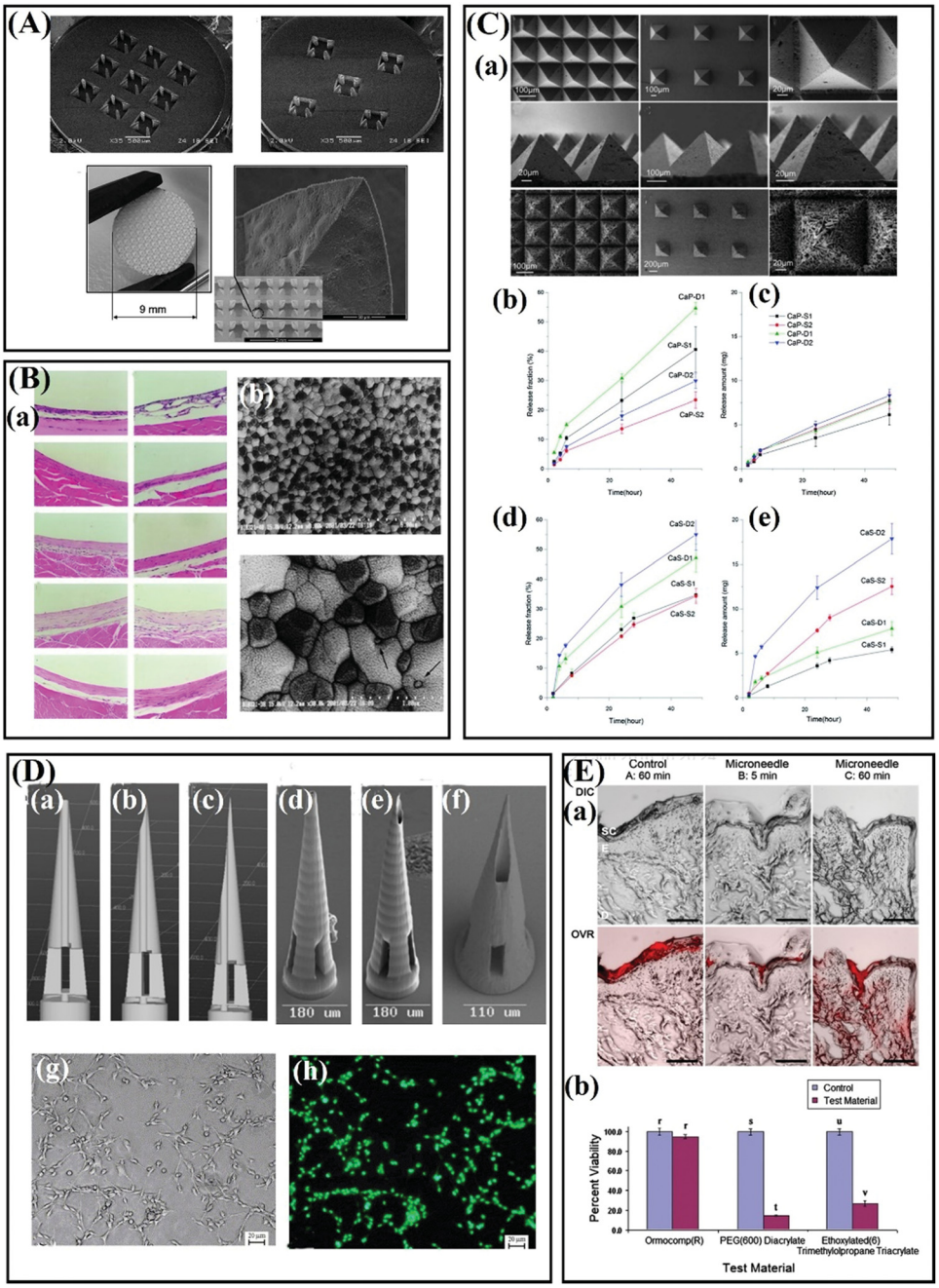

Fig. 5 (A) Overview images and detailed scanning electron micrographs of alumina-based nanoporous ceramic MNs. Adapted with permission from ref. 57. Copyright 2015 Elsevier. (B) (a)Tissue response around tested materials. (b) Scanning electron micrographs of Ce-TZP/Al_2O_3 nanocomposite after thermal etching. Adapted with permission from ref. 59. Copyright 2002 John Wiley and Sons. (C) (a) SEM images: top view of intact calcium sulfate (CaS) MNs. (b) Fraction of drug released *versus* time and (c) amount of drug released *versus* time from CaP SCMNs with zolpidem tartrate integrated into the matrix. (d) Fraction of drug released *versus* time and (e) amount of drug released *versus* time for CaS SCMNs with zolpidem tartrate integrated into the matrix. Adapted with permission from ref. 63. Copyright 2012 Royal Society of Chemistry. (D) Computer-aided design diagrams of MNs with (a) 0 μm, (b) 1.4 μm, and (c) 20.4 μm pore–needle center displacement values. Scanning electron micrographs of Ormocer® MNs with (d) 0 μm, (e) 1.4 μm, and (f) 20.4 μm pore–needle center displacement values. Adapted with permission from ref. 66. Copyright 2007 John Wiley and Sons. (g) Optical micrograph and (b) fluorescence micrograph of live/dead assay-stained B35 neuroblast-like cells on an Ormocer® surface 48 h after inoculation. Adapted with permission from ref. 65. Copyright 2006 Elsevier. (E) MTT viability of human epidermal keratinocytes on Ormocomp®, PEG (600) diacrylate, and ethoxylated (6) trimethylolpropane triacrylate surfaces relative to paired controls. Adapted with permission from ref. 68. Copyright 2010 American Scientific Publishers.

the loaded ovalbumin (OVA) could be released from the self-setting MNs (600 μm-tall) within 1 h.[64]

Also, Ormocer® materials, a kind of amorphous organic–inorganic hybrid material, have also been developed for the

preparation of MNs.[65,66] The special crossed-linked 3 D network provides Ormocer® materials with exceptional properties such as chemical and thermal stability.[65] Generally, the Ormocer® materials-based MNs are fabricated by two photon polymerization (2PP), and the MNs have good biocompatibility (Fig. 5D and E).[65–68] Ovsianikov *et al.* successfully prepared hollow MNs using 2PP technology based on Ormocer® US-S4 material.[66] The study demonstrated that the Ormocer®-based MNs strong enough to penetrate porcine skin without fracture, and this material almost does not affect the growth of human epidermal keratinocytes.[66]

2.4. Metal

Numerous metals and their alloys, such as stainless steel,[69] titanium,[70] palladium,[71] nickel,[72] tungsten,[73] gold and silver,[74,75] have been developed for the fabrication of MNs due to their excellent mechanical properties such as high Young's moduli and tensile strength. Compared with glass and silicon MNs, the preparation method of metallic MNs is more diverse and the cost is relatively lower. Two main approaches are used in the fabrication of metal MNs and electrodeposition metallic MNs.

Stainless-steel and titanium are the commonly used materials for the fabrication of metallic MNs due to their biocompatibility and excellent mechanical properties.[76,77] In fact, stainless-steel (316L) and titanium have been widely used for biomedical devices such as orthopedic and dental implants for many years.[78] Both of these two metals may suffer from corrosion in bodies and cause adverse effects such as chronic allergy after long-term implantation.[48,78] However, the administration of metal MN is usually completed in a short time, so there is almost no need to worry about them being corroded. Besides, stainless steel (316L) and titanium can be used to prepare porous metallic MNs for biosensing and drug delivery (Fig. 6A).[22,79,80] Palladium and nickel are commonly used materials for preparing hollow metallic MNs by electrodeposition (Fig. 6B).[81,82] Briefly, the sacrificial structure MNs with a sputter-deposited seed layer are prepared first, then palladium or nickel materials are coated on the surface of the MNs by electrodeposition, and finally the sacrificial structure MNs are removed to form hollow MNs (Fig. 6C).[83–85] In addition to its good mechanical properties, electroplated palladium is also a biologically inert material with good biocompatibility.[83] However, it should be noted that nickel is not a biocompatible material and is even considered as a carcinogenic material.[84,86] To avoid the safety issues such as skin irritation or toxicity caused by nickel, the outermost layer of nickel-based MNs are usually coated with a layer of biocompatible materials, such as palladium, silver or gold, to eliminate nickel exposure.[74,87] Besides, the noble metals of silver and gold are generally used as the outermost layer of MNs for various purposes, such as improving the compatibility of MNs or for antibacterial or biosensors.[67,75]

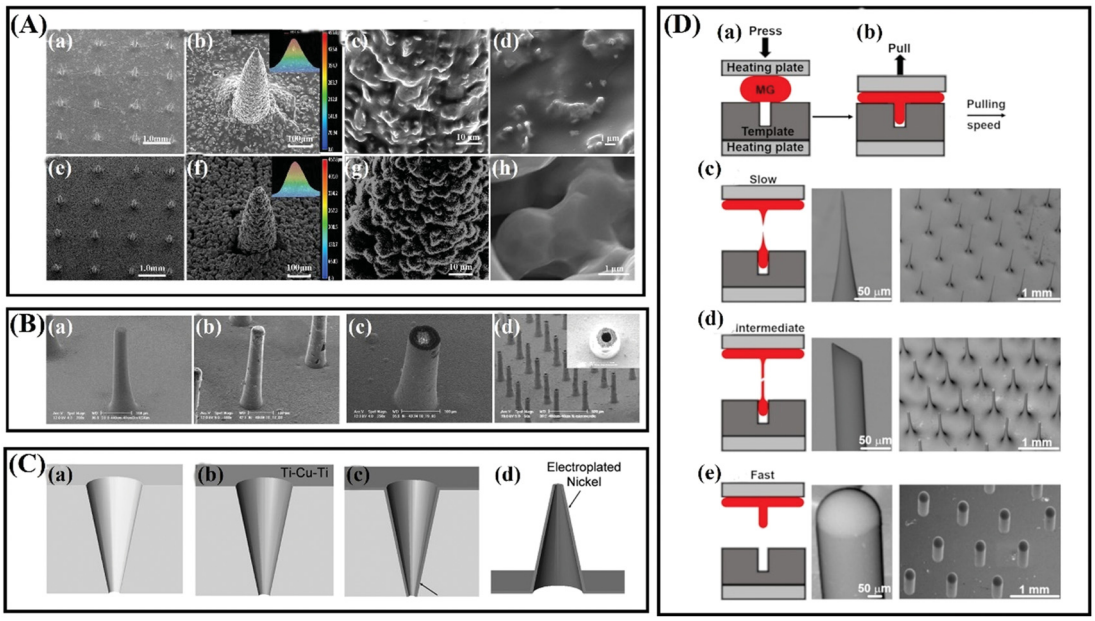

Fig. 6 (A) The morphology of (a–d) titanium microneedle array (TMA) green body and (e–h) titanium porous microneedle array (TPMA). Adapted with permission from ref. 80. Copyright 2017 Public Library of Science. (B) SEM photomicrographs of a hollow metallic MNs array under fabrication: (a) 400 μm tall tapered SU-8 pillar; (b) electroplated nickel covered SU-8 pillar; (c) an opened MNs tip after SU-8 planarization and polishing; (d) 400 μm tall metallic hollow MNs array with 20 μm in wall thickness. Adapted with permission from ref. 82. Copyright 2006 Springer Nature. (C) Schematic sequence of the MNs fabrication process using a polymer mold: (a) tapered holes are laser drilled through a polymer substrate, (b) a conductive seed layer is deposited on the top and sidewalls of the mold, (c) metal is electroplated onto the seed layer and (d) the mold is selectively wet etched to release the metal MNs. Adapted with permission from ref. 84. Copyright 2005 IEEE. (D) Fabrication of MNs using thermoplastic drawing of Pt-based MG. (a) MG is heated and embossed into a template cavity. (b) MG fiber is drawn from the cavity at different speeds while keeping the temperature constant. (c) MG fiber necks and breaks into conical MNs at a slow pulling speed. (d) A nearly uniform MG fiber is drawn at an intermediate speed, which is fractured at room temperature to create bevel shaped MNs. (e) At a fast pulling speed, the MG separates from the cavity resulting in the formation of the parabolic tip profile. Adapted with permission from ref. 88. Copyright 2020 AIP Publishing.

Table 1 Matrix materials for fabrication of silicon, glass, ceramic and metallic MNs

Materials	Young's modulus (GPa)	Advantages	Limitations	Examples	Ref.
Silicon	130–188	Excellent mechanical strength Can be used to design a variety of desirable shapes	Inherently brittle Relatively expensive Fractured silicon fragments remaining under the skin may endanger health	Solid MNs to enhance drug delivery	32, 34, 36, 38, 41
Glass	39–66 (borosilicate glass)	Cheap, transparent, chemical inertness Borosilicate glass appears to be biocompatible with the cortical surface	Inherently brittle Typically manufactured by hand, which is not time efficient Silica glass may cause granulomas in the skin	Hollow MNs for insulin delivery	25, 41–43, 46
Alumina ceramics	—	Controlled porosity Chemical and thermal stability Biocompatible	Inherently brittle High processing temperature	Solid MNs for vaccine delivery	26, 51, 57–59
Gypsum and brushite	—	Good mechanical strength Resorbable, biocompatible, degradable Self-setting under room condition	Inherently brittle	Controlled release of zolpidem	62,63
Ormocer®	17	Sufficient mechanical strength Good toughness Chemical and thermal stability Nontoxic and biologically inert	Usually fabricated by 2PP, thus the residue of the photoinitiator should be considered	For fabrication of hollow MNs and solid MNs	65–67
Stainless-steel	180–220	Conductivity Excellent toughness and mechanical properties	May suffer from corrosion in bodies after a long-term implantation	For vaccine delivery	48, 69, 78
Titanium	115	Excellent toughness and mechanical properties Excellent biocompatibility Non-toxic	Expensive	Porous Ti MNs for continuous insulin delivery	70, 78, 79
Palladium	117	High mechanical strength and ductility Biocompatibility	Expensive	For the fabrication of hollow MNs	5, 71, 83
Nickel	~207	Inexpensive Good mechanical strength and durability	Potential carcinogenic nature: nickel has been found to cause allergic reactions upon skin contact in some people	Hollow MNs for insulin delivery to diabetic Rats	84, 86, 89
Tungsten	—	Excellent tensile strength, good conductivity, relative chemical inertness, and antiradiation qualities Low toxicity	Poor ductility Potential health effects of tungsten remain to be fully defined	Tungsten MNs are used to insert neural electrodes into living peripheral nerves	73, 90

Generally, these traditionally metallic MNs described above are generally fabricated by laser cutting, etching, or electrodeposition. These fabrication processes are usually complex or multi-step. Recently, Hu and colleagues proposed a new idea for the preparation of solid and hollow metallic MNs using a thermoplastic drawing of metallic glasses (Fig. 6D).[88] This study also demonstrated that both metallic glass MNs are strong enough to pierce porcine skin and deliver model drugs.[88] Metallic glasses are such metals that not only exhibit good mechanical properties like conventional metals but also can be molded like polymers.[88] There is no doubt that this kind of metallic glass provides a convenient way for the fabrication of metallic MNs, especially for hollow metallic MNs. The properties of silicon, glass, ceramic and metal discussed above are shown in Table 1.

2.5. Oligosaccharides

Oligosaccharides have the advantages of low cost, low toxicity, and excellent biocompatibility, which are ideal materials for the preparation of MNs (Table 2). Compared with the silicon, ceramic, glass and metal materials discussed above, most oligosaccharides are water-soluble and basically safe for human health. Therefore, the MNs fabricated by such carbohydrates will dissolve after contacting ISF and leave behind no sharp, biohazardous waste. Also, oligosaccharide-based MNs can be easily fabricated by the micromolding technique.

One of the commonly used oligosaccharides for the fabrication of MNs is maltose (Fig. 7A).[91–93] Miyano *et al.* fabricated an array of maltose MNs of lengths ranging from 150 μm to 2 mm for the transdermal application of dye and cosmetics.[93] Briefly, powdered maltose was first heated at 140 °C and uniformly mixed up with drugs, then the mixture was put on the needle-shaped casting mold at 95 °C to cast into MNs, and finally the MNs obtained by demolding after cooling the mold.[93] The results showed that the maltose MNs have enough strength to pierce the skin and are safe for the human skin in a short-term.[93] Kolli and Banga also proved that the maltose MNs are strong enough to penetrate the skin to enhance drug

Table 2 Several commonly used matrix materials for the fabrication of polymer and carbohydrate MNs

Materials	Insertion ability	Dissolution/ degradation time	Safety	Limitations	Ref.
Maltose	Sufficient mechanical strength to pierce the healthy human skin (500 μm-tall)	Dissolved in 5 min in human skin	Biocompatible No dermatological problems were observed on the human skin after insertion.	High melting point is not good for heat-labile drugs and poor moisture resistance limited the use of MN in a humid environment.	92, 93
Hyaluronic acid (HA)	Tips were sharp enough to breach the stratum corneum into the dermis of the skin (conical, ~600 μm-tall, 300 μm-base diameter).	Dissolved in 2 min in porcine cadaver skin (HA, Mw = 35 kDa)	FDA-approved Biocompatible, biodegradable Nontoxic and nonirritant Hypersensitivity effects or side effects of HA MNs were not found in clinical studies	Poor moisture resistance, easy to shrink the fabrication of MNs.	124, 184, 185
Carboxymethylcellulose (CMC)	Predicted fracture force is about 0.65 N per needle. (~670 μm-tall, 376 μm base diameter, and 63 μm-tip diameter).	Dissolved in 5 min in rat skin completely.	FDA-approved materials Biocompatible, biodegradable No side effects were observed *in vitro* cytotoxicity analysis and *in vivo* tissue response test after treatment by CMC MNs.	Poor moisture resistance	21, 186
Poly(vinylpyrrolidone) (PVP)	Sufficient strength to penetrate the mice skin (pyramidal, 800 μm-tall).	Dissolved in 5 min in mice skin.	Biocompatible, biodegradable Low oral and transdermal toxicity Non-irritating to skin No treatment-related adverse effects were seen in a 6-month study in which bolus doses of 4800 mg PVP kg^{-1} (gavage).	Poor moisture resistance limited the use of MN in a humid environment.	106, 123, 127, 134, 187
Polyvinyl alcohol (PVA)	Enough strong to pierce the porcine cadaver skin and mice skin (conical, ~600 μm-tall, 300 μm-base diameter).	Dissolved in 2 min in porcine cadaver skin.	FDA-approved material Biocompatible, biodegradable Low cytotoxicity MNs fabricated with PVA and sucrose (1 : 1) are well tolerated in the skin with mild erythema but resolved within 7 days.	Poor moisture resistance limited the use of MN in a humid environment.	108, 128, 188
Amylopectin	Predicted failure force is 0.93 N per needle (conical, 600 μm-tall, 300 μm-base diameter).	Dissolved more slowly than PVP.	Non-cytotoxic Biocompatible, biodegradable	—	115
PMVE/MA PMVE/MAH	An insertion force of 0.089 N per needle for 30 s is enough to penetrate neonatal porcine skin (Gantrez® S-97).	Dissolved in 40 min in porcine skin and 60 min in murine skin. (Gantrez® AN119)	Non-cytotoxic Biocompatible, biodegradable Repeat application of PMVE/MA MN does not cause skin immunity or problems in mice *in vivo* (Gantrez® S-97 BF).		112, 127, 136, 137, 189
Silk fibroin	Sufficient mechanical strength to penetrate mice skin for drug delivery.	Varies from several hours to several days.	FDA-approved biomaterial Non-cytotoxic Biocompatible and the *in vivo* degradation products are non-inflammatory.	Long fabrication time	116, 141
Polylactic acid (PLA)	Excellent mechanical strength to penetrate the porcine cadaver skin (conical, 600 μm-tall).	—	FDA-approved biomaterial for the use of implants in humans. Biocompatible, biodegradable The *in vivo* degradation products are nontoxic.	High fabrication temperature (over 170 °C) or organic solvents are usually required for the fabrication of MNs.	158, 159

Table 2 (*continued*)

Materials	Insertion ability	Dissolution/ degradation time	Safety	Limitations	Ref.
Polyglycolic acid (PGA)	Excellent mechanical strength to penetrate the regenerated human skin (conical, 642 μm-tall).	—	FDA-approved biomaterial for use in implants in humans. Biocompatible, biodegradable The *in vivo* degradation products are nontoxic.	High fabrication temperature or organic solvents are usually required for the fabrication of MNs.	149
Poly(lactide-*co*-glycolic acid) (PLGA)	Excellent mechanical strength to penetrate and pierce the murine skin (conical, 700 μm-tall and 250 μm-base width).	Degradation time is related to the ratio of a monomer of lactic and glycolic acid, usually over 28 days.	FDA-approved biomaterial Biocompatible, biodegradable The *in vivo* degradation products are nontoxic.	High fabrication temperature or organic solvents are usually required for the fabrication of MNs.	158, 160, 161
Polycaprolactone (PCL)	Sufficient mechanical strength to penetrate porcine cadaver skin for drug delivery.	Varies from several days to several months.	FDA-approved biomaterial for use in implants in humans. Non-cytotoxic Biocompatible, biodegradable The *in vivo* degradation products are nontoxic.	The process temperature is relatively lower than PLA, PGA and PLA, but still over 50 °C, which is limiting for the incorporation of heat-labile medicaments such as insulin.	158, 162
Chitosan	Sufficient mechanical strength to penetrate porcine cadaver skin (600 μm-tall, 250 μm-base width).	Can be degraded within 30 days.	Biocompatible, biodegradable and nontoxic Can be cleared by the kidneys *in vivo* or degraded into fragments and then cleared by the kidneys.	Limited raw materials	167, 190

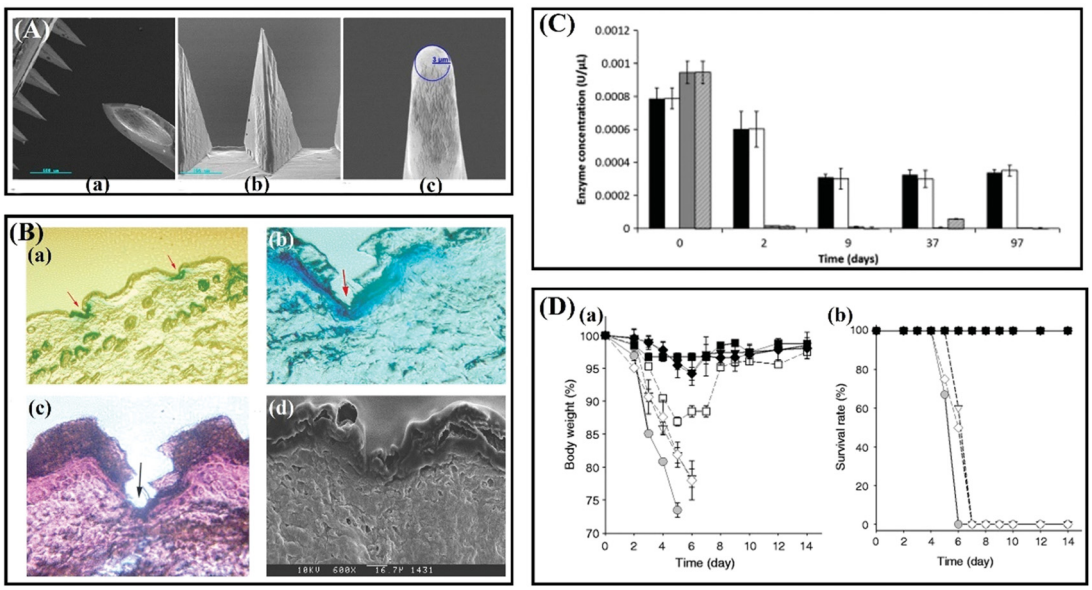

Fig. 7 (A) Scanning electron micrograph image of 500 μm long solid maltose MNs shown (a) in an individual array (b) and magnified view that shows the radius of the tip (c). Adapted with permission from ref. 91. Copyright 2007 Springer Nature. (B) (a) Histology of unstained cryosection of MN streated rat skin, in magnified view. (b) H&E-stained cryosection following pretreatment. (c) Blue at the bottom of the pore indicates the methylene blue staining. (d) SEM image of skin section following treatment with MNs. Adapted with permission from ref. 92. Copyright 2009 Elsevier. (C) Assessment of biomolecule stability within sugar glasses. Samples were stored under vacuum desiccation at 20 ± 2 °C (white and striped bars) or desiccation at 4 ± 2 °C (black and grey bars) for a period of 3 months. Residual enzyme activity was quantified at time points by 2-nitrophenyl β-D-galactopyranoside assay. Adapted with permission from ref. 95. Copyright 2012 Elsevier. (D) Protective efficacy of influenza vaccine coated onto MNs after drying and storage. (a) Body weight and (b) survival rate of immunized mice after lethal challenge infection with 20 × LD50 A/PR8/34 live virus. MNs storage was at 25 °C. (n = 6 replicates expressed as average ± SEM). Adapted with permission from ref. 96. Copyright 2013 Elsevier.

delivery (Fig. 7B).[91] There is no doubt that the mold-based fabrication technique is simple, low cost, and easy to mass produce. However, it is worth noting that maltose needs to be melted at a high temperature before casting and drug loading, so the drugs mixed with maltose should have sufficient heat resistance to maintain their pharmacological activities. Obviously, temperature-sensitive drugs, such as insulin and vaccines, are easily degraded and lost their pharmacological activities at such a high fabrication temperature. Galactose MNs also need to be heated during the process.[94] Based on these issues, Martin *et al.* investigated the feasibility of using a low temperature processing method (50 °C) to produce biodegradable MNs with sugar glasses.[95] The results demonstrated that this kind of sugar MN has sufficient structural rigidity to efficiently penetrate excised human breast skin (Fig. 7C).[95] Besides, sucrose and trehalose are commonly used in the fabrication of MNs acting as a stabilizer to protect drugs or as additives to allow the MNs to dissolve quickly (Fig. 7D).[96,97]

From the perspective of safety, oligosaccharides are the ideal materials for the fabrication of dissolving MNs. However, studies have shown that oligosaccharides MNs are easily deformed in a short time due to water absorption when exposed to ambient conditions,[94] such disadvantages are likely to make them unfavorable for clinical application.

2.6. Polymers

Ideal matrix materials of MNs should be mechanically strong, economical, biocompatible, biodegradable, have low toxicity, and should not cause skin irritation or a threat to the immune system. Polymers can provide advantages for the demanding requirements of MNs.[98–100] Besides, the structure or molecular weight of polymers can be customized according to the different application purposes (Table 2). For example, some water-soluble polymers can be designed for the rapid release of drugs,[101] while some polymers with degradable properties can be used for controlled release of drugs.[102] Polymeric MNs can be easily prepared by low-cost and easy-to-mass-produce fabrication methods such as micromolding[103] or 3D-printing.[104] Nowadays, polymers are the most commonly used matrix materials for preparing MNs.[44,105] Polymeric MNs can be generally divided into the following categories according to their drug delivery mechanism: (1) dissolving polymeric MNs (2) biodegradable MNs; and (3) hydrogel-forming MNs.

2.6.1. Dissolving polymeric MNs. Dissolving polymeric MNs are usually prepared by micromolding under vacuum or centrifugation (without heating), and facilitate the packaging of temperature-sensitive drugs. To date, various soluble polymers have been reported to fabricate dissolving polymeric MNs: typically including poly(vinylpyrrolidone) (PVP),[106] polyvinyl alcohol (PVA),[107] hyaluronic acid (HA),[108] hydroxypropyl cellulose (HPC),[109] hydroxypropyl methylcellulose (HPMC),[110] copolymers of methyl–vinyl–ether-*co*-maleic anhydride (Gantrez® AN-139, Gantrez® AN-119, Gantrez® S-97),[111–113] poly(acrylic acid) (PAA)[114] and natural polymers such as carboxymethylcellulose (CMC),[21] amylopectin,[115] silk fibroin,[116] pullulan,[117] sodium alginate,[118] dextran,[119] gelatin[120] and chondroitin sulfate.[121] These materials will dissolve quickly after contact with ISF, which provides an alternative for the preparation of rapid drug released MNs.

Among these materials, PVP, PVA, HA, CMC and their mixtures, such as PVP/PVA,[122] PVP/HA[123] and CMC/HA,[124] are the most commonly used materials for preparing dissolving MNs and have been widely studied for delivery of various drugs including small molecules, proteins or vaccines.[105,120,125] In fact, PVA and PVP have been used in numerous biomedical applications for many years because they are extremely low cytotoxicity, water-soluble, biodegradable and biocompatible.[126] Safety studies carried out by Donnelly *et al.*[127] and Zhang *et al.*[128] showed that long-term use of PVP MNs and PVA MNs on mice will not cause undesirable side-effects such as skin irritation and physiological toxicity. HA has made great contributions to the biomedical applications and cosmetics industries due to its properties of biocompatibility, biodegradability, non-immunogenicity, non-toxicity and high-water retention.[129,130] Studies have shown that HA MNs are strong enough to penetrate the skin and show great potential in drug delivery and cosmetics.[131–133] An important clinical study showed the drug-loaded MNs were applied to the crow's feet of female subjects for 8 weeks, and the wrinkles significant disappeared after 4 weeks.[134]

Another potential polymer that has proved to be highly suitable for the preparation of MNs is Gantrez® polymers including Gantrez® AN-139, Gantrez® AN-119 and Gantrez® S-97, copolymers of methyl–vinyl–ether–maleic anhydride (PMVE/MA), which are biocompatible, biodegradable, non-cytotoxic and has immunoadjuvant properties.[113,135–138] A meaningful *in vivo* study carried out by Donnelly and colleagues demonstrated that after multiple treatments of mice with Gantrez® S-97-based MNs, no measurable levels of tumor necrosis factor-α were found in any mice (Fig. 8A).[127] Pastor *et al.*[112] fabricated a series of vaccine loaded MNs based on the three polymers (Gantrez® AN-139, Gantrez® AN-119 and Gantrez® S-97) for intradermal immunization. Comparative immunization and protection results showed there were no significant differences between these three polymers.[112] Silk fibroin is also a promising polymeric material for MN fabrication due to its good toughness, mechanical strength and biocompatibility, and its degradation products *in vivo* are also non-inflammatory. Meniel *et al.* discovered that cell proliferation was significantly higher on the silk films after 96 h as compared to tissue culture plastic or collagen (Fig. 8B).[139,140] For the first time, Tsioris *et al.* used silk fibroin as the matrix material of MNs and the research showed that these MNs with excellent strength can successfully pierce the mouse skin, and can realize the continuous release of drugs (Fig. 8C).[116] Subsequently, silk fibroin MNs have been widely developed for the delivery of drugs, especially for macromolecular drugs such as vaccines[141] and insulin.[142] Additionally, these soluble polymers also can be used as the coating matrix materials for coated MNs.[143–145] However, it is a challenge for these dissolving polymer MNs while they are used in humid environments due to their highly hydrophilic nature.[146]

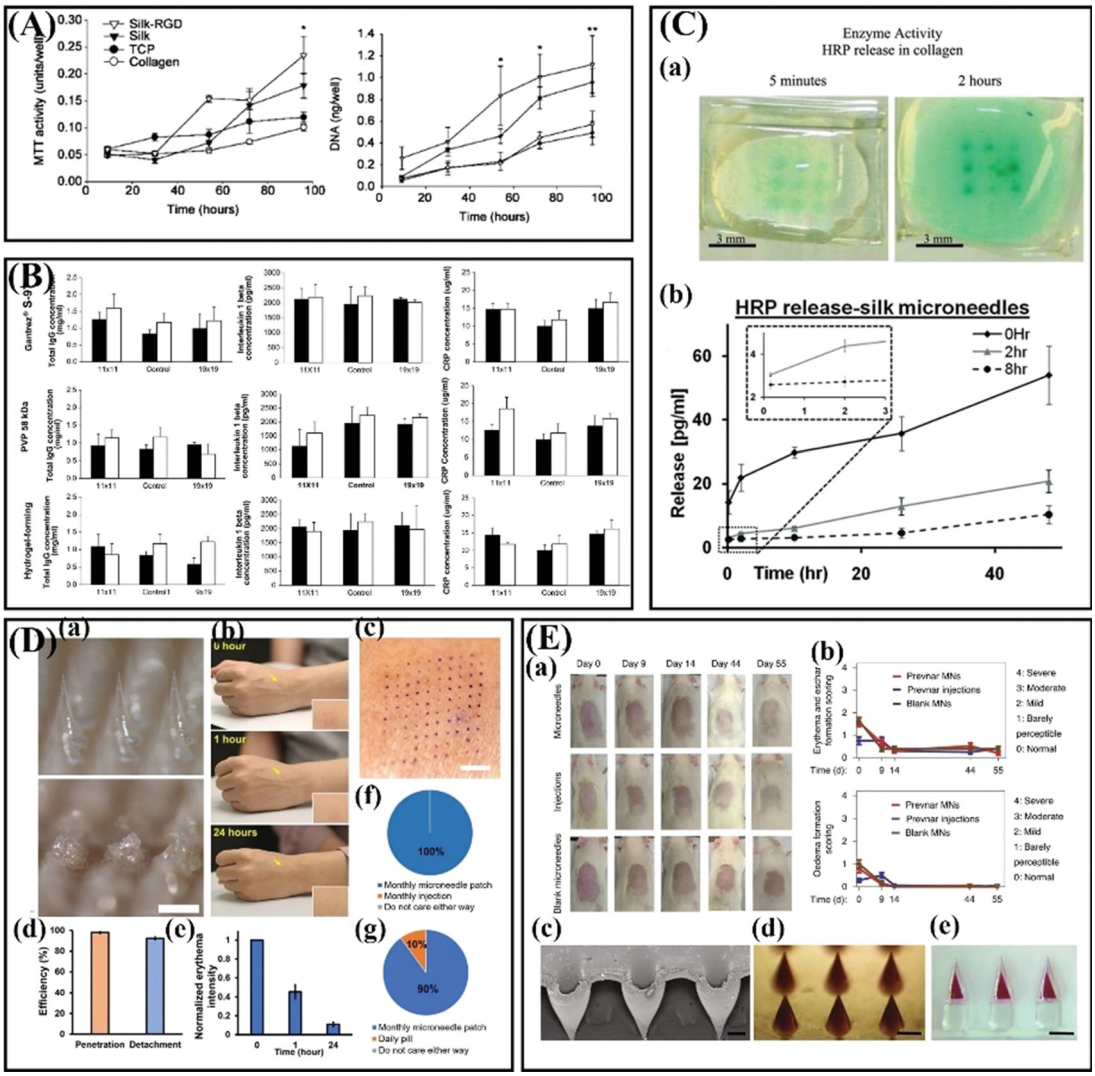

Fig. 8 (A) Serum biomarker levels of each MN-treated group. Adapted with permission from ref. 140. Copyright 2005 Elsevier. (B) DNA content per well on silk-RGD, silk, collagen films and on tissue culture plastic (TCP) after 9, 30, 54, 72, and 96 h. Adapted with permission from ref. 116. Copyright 2011 John Wiley and Sons. (C) Bioactivity of microneedle released HRP into the collagen slab after 5 min and 2 h release detected by a chromogenic substrate. (b) Total model drug release of silk MNs in collagen hydrogels, as determined from collagenase digestion and absorption spectroscopy with the insert depicting the early events of release. Adapted with permission from ref. 116. Copyright 2011 John Wiley and Sons. (D) Application of effervescent MN patches to human participants. (a) Bright-field microscopy images of an effervescent MN patch before (top) and after (bottom) application to human skin. (b) Representative images of the site of effervescent MN patch application to the skin of a human over time. (c) Representative photographic image of skin on a human participant stained to show where a 10 × 10 array of MNs punctured into the skin. (d) The efficiency of penetration and detachment of effervescent MN patches in the skin of human participants. (e) Normalized erythema intensity of human skin over time at the site of effervescent MN patch application. (f) Preference of human participants for monthly application of effervescent MN patch compared to monthly hypodermic injection for delivery of contraceptive (n = 10). (g) Preference of human participants for monthly application of effervescent MN patch compared to daily oral administration by pill for delivery of contraceptive (n = 10). Adapted with permission from ref. 160. Copyright 2019 American Association for the Advancement of Science. (E) (a) Optical images of the skin of rats from groups that received the Prevnar-13 core–shell MNs, s.c. injections and blank MNs. (b) Erythema and eschar formation on the skin of the rats was scored. (c) Oedema formation on the skin of the rats was scored. (d) SEM image of the cores of the MNs after the impinging step. (e) Optical image of fabricated core drugs inside the PVP matrix. (f) Optical image of the drug-loaded core–shell MNs after the manufacturing process. Adapted with permission from ref. 161. Copyright 2020 Springer Nature.

2.6.2. Biodegradable MNs. Compared with the traditional metallic, glass and silicon MNs discussed above, biodegradable MNs are generally fabricated by biodegradable polymers with good biocompatibility and non-toxicity. Biodegradable MNs can be used not only for skin pretreatment, but also can be used as the internal support part of coated MNs. Importantly, they can provide a good platform for the sustained release of drugs. The representative matrix materials of biodegradable MNs are polylactic acid (PLA),[147,148] polyglycolic acid (PGA)[149] and poly(lactide-*co*-glycolic acid) (PLGA),[150] polycaprolactone (PCL),[151] chitin and chitosan.[152–154]

As for PLA, PGA, PLGA, and PCL, they are all FDA approved polyesters and have been used as implants for decades due to their favorable mechanical properties and ability to be degraded

into non-toxic products in a physiological environment.[155–158] On the other hand, they can melt under heating or dissolve in an organic solvent, which makes them suitable for the preparation of MNs. Li *et al.*[159] proved that the excellent mechanical properties of the PLA MN patch enable it to penetrate pig skin after repeated use and this patch have the potential to enhance the transdermal delivery of insulin. Prausnitz and colleagues designed an effervescent MN patch based on PLGA for long-acting reversible contraception, and both *in vitro* and *in vivo* results showed that this MN patch can slowly release levonorgestrel over 1 month, and the insertion of the MN patch did not cause adverse reactions (Fig. 8D).[160] Tran and coworkers proposed a kind of core–shell structured MN based on PLGA for delayed burst release of vaccines. The safety of these PLGA MNs was evaluated from the skin edema after micro acupuncture (Fig. 8E).[161] Briefly, the shells are fabricated by PLGAs with different degrees of degradation and thus the shells can be degraded at different time points to burst release the vaccines loaded in the cores.[161] Similarly, PCL also can be used to prepare biodegradable MNs by combining with some soluble polymers for sustained release of drugs.[162] Additionally, PCL can be used as the matrix material of near-infrared light triggered MNs for thermally triggered drug release due to its relatively low melting point (59–64 °C).[162–165]

All these studies described above showed the potential of these polyester-based MNs for sustained drug release. However, organic solvents are usually required to dissolve these materials to mix them with drugs during the preparation of polyester-based MNs. There is no doubt that the residual organic solvents may cause toxicity problems for such polyester-based MNs. Thus, chin and its derivative chitosan are proposed as potential materials for the fabrication of biodegradable MNs because of their mild formulation process, physiologically inert, biodegradable and non-toxic.[152,153,166] Chiu and coworkers developed HA/chitosan composite MNs for single-dose intradermal immunization.[167] The results demonstrated that the chitosan base embedded in the skin can release antigen continuously for up to 4 weeks, and the chitosan base can be gradually degraded within 30 days.[167] Besides, some cross-linked polymers such as gelatin methacryloyl (GelMA) or methanol treated silk fibroin are also used as the matrix materials of MNs for the controlled release of drugs.[168–170] However, the matrix materials of both

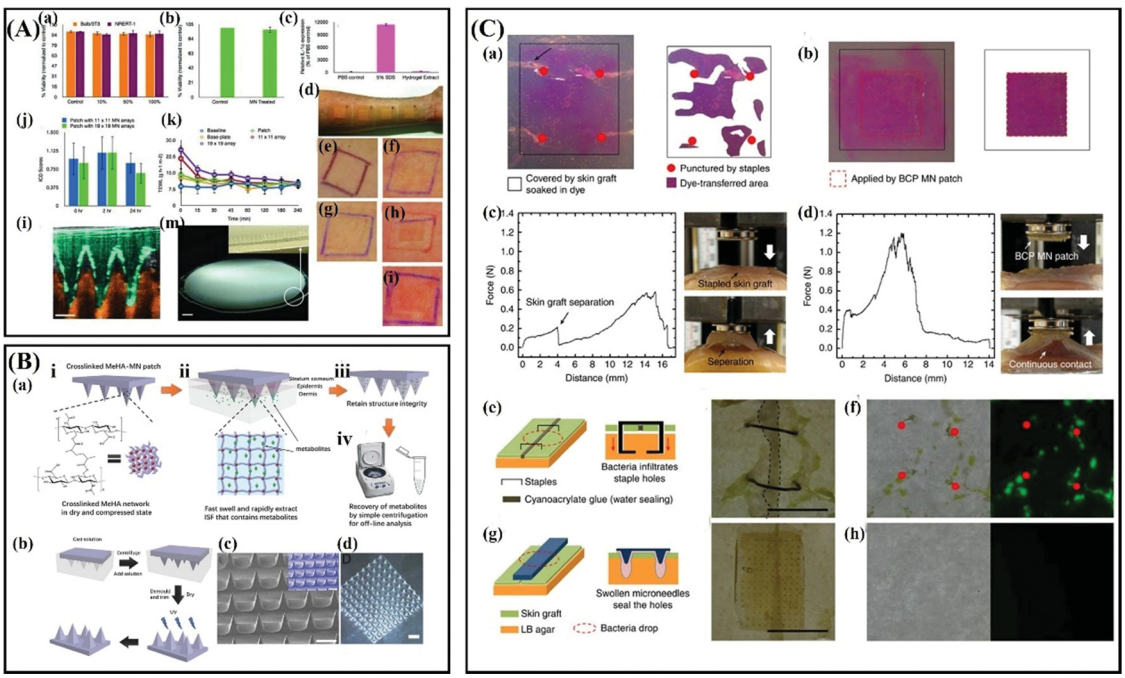

Fig. 9 (A) *In vitro* and *in vivo* safety studies for hydrogel-forming MNs. (a–c) Results of cytotoxicity studies in cell lines. (d) A representative pattern of application of four different plasters on the ventral forearms of human volunteers. (e–i) Representative samples of clinical photographs taken to measure the ICD scores in human volunteers in a 24 h treatment group by expert dermatologists. (j) The mean ICD scores in human volunteers following removal of the two different densities of hydrogel-forming MN array in the 24 h treatment group. (k) Mean TEWL values following removal of hydrogel-forming MN array in the 24 h treatment group. (l) An OCT image 2 h following insertion of hydrogel-forming MN array (height 600 μm, width at base 300 μm, spacing 300 μm, 11 × 11 arrays) into human skin *in vivo*. (m) a digital image of a hydrogel-forming MN array containing approximately 18 000 MN needles in a 25 cm^2 area, the hydrogel needles can be seen in the inset. Adapted with permission from ref. 173. Copyright 2012 John Wiley and Sons. (B) (a) Schematic representation of the rapid extraction of ISF by crosslinked MeHA-MN patches. (b) Schematic of the fabrication process of crosslinked MeHA-MN patch. (c) Scanning electron microscopy (SEM) image of crosslinked MeHA-MN patch, the inlet is a false-color image. (d) Optical image of crosslinked MeHA-MN patch. Scale bar is 1000 μm. Adapted with permission from ref. 177. Copyright 2017 John Wiley and Sons. (C) (a,b) Comparison of the contact area between a skin graft and tissue-like hydrogel (4 wt% agarose gel) after (a) applying staples and (b) a BCP MN adhesive. (c and d) Force-displacement profiles and photographs acquired during pull-off tests of the skin graft on muscle tissue fixed by (c) staples and (d) BCP MN adhesive. (e–h) Comparison of the bacterial barrier property of incised skin grafts following application of (e,f) staples and (g,h) a BCP MN adhesive. Adapted with permission from ref. 182. Copyright 2013 Springer Nature.

dissolving polymer MNs and biodegradable MNs will also leave in the skin after administration, which is unfriendly to patients, especially for patients who need long-term administration. Therefore, whether these types of MNs will cause adverse reactions in the body after long-term use is also an urgent research topic.

2.6.3. Hydrogel-forming MNs. Unlike dissolving MNs or biodegradable MNs, hydrogel-forming MNs can swell in the skin and can be removed completely from the skin after application due to their 3D network structure. Such MNs have been developed for various biological applications including ISF extraction, wound healing and sustained drug delivery.[171,172] Generally, hydrogel-forming MNs are fabricated by biocompatible cross-linked polymers, typically including cross-linked poly(methyl-vinylether/maelic acid) (PMVE/MA), HA, PVA.

For the first time, Donnelly and coworkers successfully prepared hydrogel-forming MNs based on poly(ethyleneglycol) (PEG, 10 000 Da) cross-linked PMVE/MA (PMVE/MA:PEG 2 : 1) in 2012.[173] The results suggested that the MNs based on this material are biocompatible, non-irritant, and no safety issues occurred among human volunteers (Fig. 9A).[173] They further proved the potential of hydrogel-forming MNs for bolus delivery of drugs and vaccines.[174] Recently, a study demonstrated that repeatedapplication of these crossed-linked PMVE/MA MNs does not lead to prolonged skin irritation or damage to the skin barrier function.[175] Also, the cross-linked PMVE/MA MNs can be used to extract ISF for analysis.[176] However, almost 1 hour is required to extract adequate ISF ($\sim$0.84 mg) due to the slow swelling rate of this MNs.[176] Based on this issue, Chang *et al.*[177] considered hyaluronic acid (HA), which is highly hydrophilic and has natural super-hydrating properties, as a candidate for microneedle matrix material. Considering also the water solubility of HA, they prepared crosslinked methacrylated hyaluronic acid (MeHA) MNs for rapidly ISF extraction. The good mechanical properties and high swelling rate allow theMeHA MNs to easily penetrate the skin and rapidly extract ISF ($\sim$1.4 mg) in 1 min.[177] These MeHA MNs have been developed for direct glucose analysis by integrating with the glucose sensor. And the results of *in vitro* and *in vivo* safety tests showed that these MeHA MNs were friendly to the human body and had good biocompatibility (Fig. 9B).[178] Additionally, PVA is also developed for the fabrication of hydrogel forming MNs due to its unique phase-transition property.[179,180] Uniquely, cross-linking of PVA hydrogel can be realized by a freeze–thaw treatment under mild process conditions without cross-linking agents.[179] Another important application of hydrogel-forming MNs is for wound healing, because the needles will swell after water absorption and thus interlock with tissue.[181,182] Typically, Yang and coworkers designed a double-layered MN array based on polystyrene-*block*-poly(acrylic acid) (PS-*b*-PAA) and the PS homopolymer.[182] Briefly, the out layer of each MN was fabricated by swellable PS-*b*-PAA and the support inner structure was fabricated by non-swellable PS homopolymer. These MNs exhibit universal adhesion to soft tissues and mechanically interlock with tissues without significant damage while providing an effective barrier to bacteria, which is a main cause of infection (Fig. 9C).[182] Besides, hydrogel forming MNs can be designed for on-demand drug delivery.[183]

In general, hydrogel forming MNs show great potential for sustained or controlled release of drugs and the ability to passively extract ISF. However, it is necessary to pay attention to the burst-release problem of the hydrogel forming MNs in the initial administration.[171] In addition to meeting the requirements of safety and mechanical properties, the degree of crosslinking of hydrogel materials is also a major factor to decide the application of hydrogel forming MNs.

3. MN products

Research on MNs is not limited to the academic field. Many companies have also developed microneedle-related products for drug and vaccine delivery or for cosmetic purposes. Some of them are summarized in Table 3. It can be seen that dissolving HA MNs are widely developed by many companies for skin blemishes treatment. The main reason may be that the safety and biocompatibility of HA materials have been extensively verified.

Table 3 Several microneedle products[191–193]

Company	Product	MN Type	Application
Becton Dickinson (BD) (USA)	Soluvia®	Hollow MNs	To deliver drugs and vaccines.
3M (USA)	Microneedle Transdermal Systems	Solid and Hollow MNs	To deliver biologics.
Corium	Corplex™	Polymer-based MNs	For treatment of Alzheimer's disease
Corium	MicroCor®	—	To deliver biologics.
CosMED Pharmaceutical (Japan)	MicroHyala®	Dissolving MNs (HA)	For wrinkle treatment.
Darmaroller® (Germany)	Dermaroller	Solid MNs (metal)	To improve skin blemishes and enhance drug absorption.
Hugel (Korea)	Wellage®	Dissolving MNs (HA)	For cosmetic purposes.
Nanomed Skincare (USA)	LiteClear®	Solid MNs (silicon)	For skin pre-treatment and skin blemishes
Nanopass Technologies (Israel)	Micronjet®	Hollow MNs	To inject liquid substances
Raphas (Korea)	Raphas®	Dissolving MNs	For cosmetic purposes and drug delivery.
Soya Greentech (Korea)	Review cell Snow White Hyaluronic Sheet	Dissolving MNs (HA)	For cosmetic purposes.
Theraject (USA)	Drugmat®	Dissolving MNs	For transdermal drug delivery
Theraject (USA)	Vaxmat®	Dissolving MNs	To deliver drugs or macromolecules
Zosano Pharma (USA)	Macroflux®	Solid MNs (metal)	To deliver peptides and vaccines.

4. Conclusion

The purpose of this review is to summarize the current matrix materials of MNs and analyze their pros and cons in terms of mechanical properties, biocompatibility and toxicity. In conclusion, MNs play a vital role in medical sciences, especially in delivering macromolecular drugs and improving skin blemishes. Up to now, various materials, including silicon, metals, glass, ceramics, carbohydrates and polymers, have been reported for the preparation of MNs.

In general, silicon can be used to design a variety of desirable MN shapes with excellent mechanical properties, but its brittle nature and uncertain biocompatibility limited its application. Metallic MNs are strong enough to penetrate the skin barrier, but their fabrication processes are usually complex or multi-step. The excellent transparency, and physically and chemically inert properties of glass make it popular in the preparation of hollow MNs. However, glass MNs also suffer from the brittle problem as silicon MNs. Ceramic MNs have aroused great interest to their outstanding properties such as porosity and biocompatibility, but the high processing temperature limits the loading of some active drugs. Oligosaccharides MNs are usually fabricated by dissolving materials with low toxicity, but their poor mechanical properties need further enhancement. Polymers are the commonly used materials for the fabrication of MNs because they can be designed for rapid drug delivery, controlled drug delivery or pain-free ISF extraction. Most of them can meet the mechanical and biocompatible requirements for MN penetration into the skin. However, to promote the clinical application of polymer MNs, lots of experiments are still needed to evaluate and ensure their drug release kinetics and safety in the body after long-term administration.

5. Perspectives

Despite the current great success of MNs in transdermal drug delivery, the long-term use of MNs remains a challenge. One of the challenges is that the size of MNs makes it difficult to achieve high dose administration. In the future, the shape of the MNs should be designed, such as funnel-shaped microneedles, while the hydrogel-forming MNs may tend to use the backing layer as the drug reservoir to increase the drug loading. In addition, the large-scale production of MNs is also limited by matrix materials. For example, glass MNs can only be prepared by the traditional method of drawing glass rods with an attractor, due to the significant chemical inertness and low chemical reactivity of glass. Metallic MNs are usually prepared by etching, and metallic MNs are not suitable for large-scale production due to the brittleness of metal materials themselves. Therefore, polymer MNs may become the mainstream MN products in the future.

At the same time although a number of MN products have appeared on the market, most of them are still only in the experimental phase and for MNs to be used on a large scale, the corresponding experiments should be supplemented. An ideal MN product should be well coordinated between good biocompatibility, mechanical properties, painless drug delivery, and high-dose administration. Also, it should be of low cost and be suitable for mass production.

Consent for publication

Written informed consent for publication was obtained from all participants.

Conflicts of interest

The authors declare that they have no conflict of interest.

Acknowledgements

This work was financially supported by the National Natural Science Foundation of China (51873015, 52161145410), the Joint Project of BRC-BC (Biomedical Translational Engineering Research Center of BUCT-CJFH) (XK2020-05, RZ2020-01), and the long-term subsidy mechanism from the Ministry of Finance and the Ministry of Education of PRC.

References

1 M. R. Prausnitz and R. Langer, *Nat. Biotechnol.*, 2008, **26**, 1261–1268, DOI: **10.1038/nbt.1504**.
2 M. Kermode, *Health Promot. Int.*, 2004, **19**, 95–103, DOI: **10.1093/heapro/dah110**.
3 A. Alexander, S. Dwivedi, G. Ajazuddin, T. K. Giri, S. Saraf, S. Saraf and D. K. Tripathi, *J. Controlled Release*, 2012, **164**, 26–40, DOI: **10.1016/j.jconrel.2012.09.017**.
4 Y. B. Choy and M. R. Prausnitz, *Pharm. Res.*, 2011, **28**, 943–948, DOI: **10.1007/s11095-010-0292-6**.
5 E. Larraneta, R. E. M. Lutton, A. D. Woolfson and R. F. Donnelly, *Mater. Sci. Eng., R*, 2016, **104**, 1–32, DOI: **10.1016/j.mser.2016.03.001**.
6 Z. M. Zhao, A. Ukidve, A. Dasgupta and S. Mitragotri, *Adv. Drug Delivery Rev.*, 2018, **127**, 3–19, DOI: **10.1016/j.addr.2018.03.010**.
7 W. D. Yao, C. H. Tao, J. F. Zou, H. Y. Zheng, J. J. Zhu, Z. H. Zhu, J. Z. Zhu, L. Liu, F. Z. Li and X. L. Song, *Int. J. Pharm.*, 2019, **563**, 91–100, DOI: **10.1016/j.ijpharm.2019.03.033**.
8 A. C. Watkinson, *J. Pharm. Sci.*, 2013, **102**, 3082–3088, DOI: **10.1002/jps.23490**.
9 Y. C. Kim, J. H. Park and M. R. Prausnitz, *Adv. Drug Delivery Rev.*, 2012, **64**, 1547–1568, DOI: **10.1016/j.addr.2012.04.005**.
10 S. Bhatnagar, K. Dave and V. V. K. Venuganti, *J. Controlled Release*, 2017, **260**, 164–182, DOI: **10.1016/j.jconrel.2017.05.029**.
11 S. Henry, D. V. McAllister, M. G. Allen and M. R. Prausnitz, *J. Pharm. Sci.*, 1998, **87**, 922–925, DOI: **10.1021/js980042+**.

12 J. Richter-Johnson, P. Kumar, Y. E. Choonara, L. C. du Toit and V. Pillay, *Expert Rev. Pharmacoecon Outcomes Res.*, 2018, **18**, 359–369, DOI: 10.1080/14737167.2018.1485100.
13 M. Jang, S. Baek, G. Kang, H. Yang, S. Kim and H. Jung, *Int. J. Cosmet. Sci.*, 2020, **42**, 302–309, DOI: 10.1111/ics.12617.
14 P. P. Samant, M. M. Niedzwiecki, N. Raviele, V. Tran, J. Mena-Lapaix, D. I. Walker, E. I. Felner, D. P. Jones, G. W. Miller and M. R. Prausnitz, *Sci. Transl. Med.*, 2020, **12**, 15, DOI: 10.1126/scitranslmed.aaw0285.
15 R. Paul, A. C. Saville, J. C. Hansel, Y. Q. Ye, C. Ball, A. Williams, X. Y. Chang, G. J. Chen, Z. Gu, J. B. Ristaino and Q. S. Wei, *ACS Nano*, 2019, **13**, 6540–6549, DOI: 10.1021/acsnano.9b00193.
16 R. F. Donnelly, K. Mooney, E. Caffarel-Salvador, B. M. Torrisi, E. Eltayib and J. C. McElnay, *Ther. Drug Monit.*, 2014, **36**, 10–17.
17 A. Muheem, F. Shakeel, M. A. Jahangir, M. Anwar, N. Mallick, G. K. Jain, M. H. Warsi and F. J. Ahmad, *Saudi Pharm. J.*, 2016, **24**, 413–428, DOI: 10.1016/j.jsps.2014.06.004.
18 K. C. Kwon, D. Verma, N. D. Singh, R. Herzog and H. Daniell, *Adv. Drug Delivery Rev.*, 2013, **65**, 782–799, DOI: 10.1016/j.addr.2012.10.005.
19 J. M. Song, Y. C. Kim, A. S. Lipatov, M. Pearton, C. T. Davis, D. G. Yoo, K. M. Park, L. M. Chen, F. S. Quan, J. C. Birchall, R. O. Donis, M. R. Prausnitz, R. W. Compans and S. M. Kang, *Clin. Vaccine Immunol.*, 2010, **17**, 1381–1389, DOI: 10.1128/CVI.00100-10.
20 J. Q. Wang, J. Yu, Y. Q. Zhang, X. D. Zhang, A. R. Kahkoska, G. J. Chen, Z. J. Wang, W. J. Sun, L. L. Cai, Z. W. Chen, C. G. Qian, Q. D. Shen, A. Khademhosseini, J. B. Buse and Z. Gu, *Sci. Adv.*, 2019, **5**, eaaw4357, DOI: 10.1126/sciadv.aaw4357.
21 B.-M. Lee, C. Lee, S. F. Lahiji, U.-W. Jung, G. Chung and H. Jung, *Pharmaceutics*, 2020, **12**, 366, DOI: 10.3390/pharmaceutics12040366.
22 E. M. Cahill, S. Keaveney, V. Stuettgen, P. Eberts, P. Ramos-Luna, N. Zhang, M. Dangol and E. D. O'Cearbhaill, *Acta Biomater.*, 2018, **80**, 401–411, DOI: 10.1016/j.actbio.2018.09.007.
23 J. Li, B. Liu, Y. Zhou, Z. Chen, L. Jiang, W. Yuan and L. Liang, *PLoS One*, 2017, **12**, e0172043, DOI: 10.1371/journal.pone.0172043.
24 B. Z. Chen, J. L. Liu, Q. Y. Li, Z. N. Wang, X. P. Zhang, C. B. Shen, Y. Cui and X. D. Guo, *ACS Appl. Bio Mater.*, 2019, **2**, 5616–5625, DOI: 10.1021/acsabm.9b00700.
25 J. Gupta, E. I. Felner and M. R. Prausnitz, *Diabetes Technol. Ther.*, 2011, **13**, 451–456, DOI: 10.1089/dia.2010.0204.
26 K. Ita, *J. Drug Delivery Sci. Technol.*, 2018, **44**, 314–322, DOI: 10.1016/j.jddst.2018.01.004.
27 K. B. Vinayakumar, G. M. Hegde, M. M. Nayak, N. S. Dinesh and K. Rajanna, *Microelectron. Eng.*, 2014, **128**, 12–18, DOI: 10.1016/j.mee.2014.05.039.
28 M. Shirkhanzadeh, *J. Mater. Sci.: Mater. Med.*, 2005, **16**, 37–45, DOI: 10.1007/s10856-005-6444-2.
29 S. Bhatnagar, A. Saju, K. D. Cheerla, S. K. Gade, P. Garg and V. V. K. Venuganti, *Drug Delivery Transl. Res.*, 2018, **8**, 473–483, DOI: 10.1007/s13346-017-0470-8.
30 L. Q. Zhang, B. Z. Chen, Y. Y. Xia, X. P. Zhang and X. D. Guo, *Sci. Adv.*, 2020, **6**, eaba7260, DOI: 10.1126/sciadv.aba7260.
31 M. Kim, B. Jung and J.-H. Park, *Biomaterials*, 2012, **33**, 668–678, DOI: 10.1016/j.biomaterials.2011.09.074.
32 M. A. Hopcroft, W. D. Nix and T. W. Kenny, *J. Microelectromech. Syst.*, 2010, **19**, 229–238, DOI: 10.1109/jmems.2009.2039697.
33 O. Paul, J. Gaspar and P. Ruther, *IEEJ Trans. Electr. Electron. Eng.*, 2007, **2**, 199–215, DOI: 10.1002/tee.20155.
34 C. O'Mahony, *Biomed. Microdevices*, 2014, **16**, 333–343, DOI: 10.1007/s10544-014-9836-6.
35 G. J. Ma and C. W. Wu, *J. Controlled Release*, 2017, **251**, 11–23, DOI: 10.1016/j.jconrel.2017.02.011.
36 S. P. Narayanan and S. Raghavan, *Int. J. Adv. Manuf. Technol.*, 2019, **104**, 3327–3333, DOI: 10.1007/s00170-018-2596-3.
37 H. E. Z. Abidin, P. C. Ooi, T. Y. Tiong, N. Marsi, A. Ismardi, M. M. Noor, N. Fathi, N. Abd Aziz, S. K. Sahari, G. Sugandi, J. Yunas, C. F. Dee, B. Y. Majlis and A. A. Hamzah, *J. Pharm. Sci.*, 2020, **109**, 2485–2492, DOI: 10.1016/j.xphs.2020.04.019.
38 S. P. Narayanan and S. Raghavan, *Int. J. Adv. Manuf. Technol.*, 2017, **93**, 407–422, DOI: 10.1007/s00170-016-9698-6.
39 R. F. Donnelly, D. I. J. Morrow, F. Fay, C. J. Scott, S. Abdelghany, R. R. T. Singh, M. J. Garland and A. D. Woolfson, *Photodiagn. Photodyn. Ther.*, 2010, **7**, 222–231, DOI: 10.1016/j.pdpdt.2010.09.001.
40 X. Jin, D. D. Zhu, B. Z. Chen, M. Ashfaq and X. D. Guo, *Adv. Drug Delivery Rev.*, 2018, **127**, 119–137, DOI: 10.1016/j.addr.2018.03.011.
41 D. V. McAllister, P. M. Wang, S. P. Davis, J. H. Park, P. J. Canatella, M. G. Allen and M. R. Prausnitz, *Proc. Natl. Acad. Sci. U. S. A.*, 2003, **100**, 13755–13760, DOI: 10.1073/pnas.2331316100.
42 P. N. Ayittey, J. S. Walker, J. J. Rice and P. P. de Tombe, *Pflugers Arch.*, 2009, **457**, 1415–1422, DOI: 10.1007/s00424-008-0605-3.
43 P. M. Wang, M. Cornwell and M. R. Prausnitz, *Diabetes Technol. Ther.*, 2005, **7**, 131–141, DOI: 10.1089/dia.2005.7.131.
44 S. Bhatnagar, P. R. Gadeela, P. Thathireddy and V. V. K. Venuganti, *J. Chem. Sci.*, 2019, **131**, 28, DOI: 10.1007/s12039-019-1666-x.
45 M. Matthaei, H. Meng, I. Bhutto, Q. G. Xu, E. Boelke, J. Hanes and A. S. Jun, *Eur. J. Med. Res.*, 2012, **17**, 6, DOI: 10.1186/2047-783x-17-19.
46 K. S. Parthasarathy, Y. C. N. Cheng, J. P. McAllister, Y. Shen, J. Li, K. Deren, E. M. Haacke and G. W. Auner, *Magn. Reson. Imaging*, 2007, **25**, 1333–1340, DOI: 10.1016/j.mri.2007.03.020.
47 Z. G. Zhu, H. Hassanin and K. Jiang, *Int. J. Adv. Manuf. Technol.*, 2010, **47**, 147–152, DOI: 10.1007/s00170-008-1864-z.
48 M. Saini, Y. Singh, P. Arora, V. Arora and K. Jain, *World J. Clin. Cases*, 2015, **3**, 52–57, DOI: 10.12998/wjcc.v3.i1.52.

49 S. M. Best, A. E. Porter, E. S. Thian and J. Huang, *J. Eur. Ceram. Soc.*, 2008, **28**, 1319–1327, DOI: 10.1016/j.jeurceramsoc.2007.12.001.
50 T. Biswal, S. K. BadJena and D. Pradhan, *Mater. Today: Proc.*, 2020, **30**, 274–282, DOI: 10.1016/j.matpr.2020.01.437.
51 S. Bystrova and R. Luttge, *Microelectron. Eng.*, 2011, **88**, 1681–1684, DOI: 10.1016/j.mee.2010.12.067.
52 M. Shirkhanzadeh, *J. Mater. Sci.: Mater. Med.*, 2005, **16**, 37–45, DOI: 10.1007/s10856-005-6444-2.
53 M. Verhoeven, S. Bystrova, L. Winnubst, H. Qureshi, T. D. de Gruijl, R. J. Scheper and R. Luttge, *Microelectron. Eng.*, 2012, **98**, 659–662, DOI: 10.1016/j.mee.2012.07.022.
54 X. H. M. Hartmann, P. van der Linde, E. Homburg, L. C. A. van Breemen, A. M. de Jong and R. Luttge, *Pharmaceutics*, 2015, **7**, 503–522, DOI: 10.3390/pharmaceutics7040503.
55 K. Ita, *J. Drug Delivery Sci. Technol.*, 2015, **29**, 16–23, DOI: 10.1016/j.jddst.2015.05.001.
56 R. Pignatello, *Biomaterials applications for nanomedicine*, 2011.
57 M. A. Boks, W. W. J. Unger, S. Engels, M. Ambrosini, Y. van Kooyk and R. Luttge, *Int. J. Pharm.*, 2015, **491**, 375–383, DOI: 10.1016/j.ijpharm.2015.06.025.
58 M. Lewandowska-Szumiel and J. Komender, *Clin. Mater.*, 1990, **5**, 167–175, DOI: 10.1016/0267-6605(90)90016-o.
59 K. Tanaka, J. Tamura, K. Kawanabe, M. Nawa, M. Oka, M. Uchida, T. Kokubo and T. Nakamura, 63, *J. Biomed. Mater. Res., Part B*, 2002, 262–270, DOI: 10.1002/jbm.10182.
60 S. Gholami, M. M. Mohebi, E. Hajizadeh-Saffar, M. H. Ghanian, I. Zarkesh and H. Baharvand, *Int. J. Pharm.*, 2019, **558**, 299–310, DOI: 10.1016/j.ijpharm.2018.12.089.
61 D. Shekhawat, A. Singh, M. K. Banerjee, T. Singh and A. Patnaik, *Ceram. Int.*, 2021, **47**, 3013–3030, DOI: 10.1016/j.ceramint.2020.09.214.
62 B. Cai, W. Xia, S. Bredenberg, H. Li and H. Engqvist, *Eur. J. Pharm. Biopharm.*, 2015, **94**, 404–410, DOI: 10.1016/j.ejpb.2015.06.016.
63 B. Cai, W. Xia, S. Bredenberg and H. Engqvist, *J. Mater. Chem. B*, 2014, **2**, 5992–5998, DOI: 10.1039/c4tb00764f.
64 H. Vallhov, W. Xia, H. Engqvist and A. Scheynius, *J. Mater. Chem. B*, 2018, **6**, 6808–6816, DOI: 10.1039/c8tb01476k.
65 A. Doraiswamy, C. Jin, R. J. Narayan, P. Mageswaran, P. Mente, R. Modi, R. Auyeung, D. B. Chrisey, A. Ovsianikov and B. Chichkov, *Acta Biomater.*, 2006, **2**, 267–275, DOI: 10.1016/j.actbio.2006.01.004.
66 A. Ovsianikov, B. Chichkov, P. Mente, N. A. Monteiro-Riviere, A. Doraiswamy and R. J. Narayan, *Int. J. Appl. Ceram. Technol.*, 2007, **4**, 22–29, DOI: 10.1111/j.1744-7402.2007.02115.x.
67 S. D. Gittard, R. J. Narayan, C. Jin, A. Ovsianikov, B. N. Chichkov, N. A. Monteiro-Riviere, S. Stafslien and B. Chisholm, *Biofabrication*, 2009, **1**, 041001, DOI: 10.1088/1758-5082/1/4/041001.
68 A. Doraiswamy, A. Ovsianikov, S. D. Gittard, N. A. Monteiro-Riviere, R. Crombez, E. Montalvo, W. Shen, B. N. Chichkov and R. J. Narayan, *J. Nanosci. Nanotechnol.*, 2010, **10**, 6305–6312, DOI: 10.1166/jnn.2010.2636.
69 Q. Y. Zhu, V. G. Zarnitsyn, L. Ye, Z. Y. Wen, Y. L. Gao, L. Pan, I. Skountzou, H. S. Gill, M. R. Prausnitz, C. L. Yang and R. W. Compans, *Proc. Natl. Acad. Sci. U. S. A.*, 2009, **106**, 7968–7973, DOI: 10.1073/pnas.0812652106.
70 G. Zhao, W. Li, G. Tang and J. Chen, Ieee, Fabrication of Bulk Titanium Out-of-plane Microneedles, in: *2009 4th Ieee International Conference on Nano/Micro Engineered and Molecular Systems*, 2009, Vol. 1 and 2, pp. 428–431.
71 J. D. Brazzle, I. Papautsky and A. B. J. B. M. Frazier, *Biomed. Microdevices*, 2000, **2**, 197–205.
72 K. Kim, D. S. Park, H. M. Lu, W. Che, K. Kim, J. B. Lee and C. H. Ahn, *J. Micromech. Microeng.*, 2004, **14**, 597–603, DOI: 10.1088/0960-1317/14/4/021.
73 S. Ma, Y. Xia, Y. Wang, K. Ren, R. Luo, L. Song, X. Chen, J. Chen and Y. Jin, *J. Vac. Sci. Technol., B: Nanotechnol. Microelectron.: Mater., Process., Meas., Phenom.*, 2016, **34**, 052002, DOI: 10.1116/1.4960715.
74 Y. Ma, C. Lee, G. Lee, Y. Cho, S.-G. Lee and H. Jung, *BioChip J.*, 2019, **13**, 394–402, DOI: 10.1007/s13206-019-3411-4.
75 S. A. Ranamukhaarachchi, C. Padeste, U. O. Hafeli, B. Stoeber and V. J. Cadarso, *J. Micromech. Microeng.*, 2018, **28**, 024002, DOI: 10.1088/1361-6439/aa9c9c.
76 E. R. Parker, M. P. Rao, K. L. Turner, C. D. Meinhart and N. C. MacDonald, *J. Microelectromech. Syst.*, 2007, **16**, 289–295, DOI: 10.1109/jmems.2007.892909.
77 M. A. Invernale, B. C. Tang, R. L. York, L. Le, D. Y. Hou and D. G. Anderson, *Adv. Healthcare Mater.*, 2014, **3**, 338–342, DOI: 10.1002/adhm.201300142.
78 Q. Chen and G. A. Thouas, *Mater. Sci. Eng., R*, 2015, **87**, 1–57, DOI: 10.1016/j.mser.2014.10.001.
79 X.-X. Yan, J.-Q. Liu, S.-D. Jiang, B. Yang and C.-S. Yang, *Micro Nano Lett.*, 2013, **8**, 906–908, DOI: 10.1049/mnl.2013.0630.
80 J. Li, B. Liu, Y. Zhou, Z. Chen, L. Jiang, W. Yuan and L. Liang, *PLoS One*, 2017, **12**, e0172043, DOI: 10.1371/journal.pone.0172043.
81 S. Chandrasekaran, J. D. Brazzle and A. B. Frazier, *J. Microelectromech. Syst.*, 2003, **12**, 281–288, DOI: 10.1109/jmems.2003.809951.
82 K. Kim and J.-B. Lee, *Microsyst. Technol.*, 2007, **13**, 231–235, DOI: 10.1007/s00542-006-0221-0.
83 S. Chandrasekaran and A. B. Frazier, *J. Microelectromech. Syst.*, 2003, **12**, 289–295, DOI: 10.1109/jmems.2003.811731.
84 S. P. Davis, W. Martanto, M. G. Allen and M. R. Prausnitz, *IEEE Trans. Biomed. Eng.*, 2005, **52**, 909–915, DOI: 10.1109/TBME.2005.845240.
85 X. Wang, X. Chen, Z. Yu and L. Wang, In: 1st IEEE International Conference on Nano/Micro Engineered and Molecular Systems, IEEE, 2006, pp. 545–549, DOI: 10.1109/NEMS.2006.334837.
86 A. Muñoz and M. Costa, *Toxicol. Appl. Pharmacol.*, 2012, **260**, 1–16, DOI: 10.1016/j.taap.2011.12.014.
87 I. Mansoor, Y. Liu, U. O. Haefeli and B. Stoeber, *J. Micromech. Microeng.*, 2013, **23**, 085011, DOI: 10.1088/0960-1317/23/8/085011.

88 Z. L. Hu, C. S. Meduri, R. S. J. Ingrole, H. S. Gill and G. Kumar, *Appl. Phys. Lett.*, 2020, **116**, 5, DOI: 10.1063/5.0008983.
89 J. D. Giallonardo, U. Erb, K. T. Aust and G. Palumbo, *Philos. Mag.*, 2011, **91**, 4594–4605, DOI: 10.1080/14786435.2011.615350.
90 P. N. Sergi, W. Jensen, S. Micera and K. Yoshida, *Med. Eng. Phys.*, 2012, **34**, 747–755, DOI: 10.1016/j.medengphy.2011.09.019.
91 C. S. Kolli and A. K. Banga, *Pharm. Res.*, 2008, **25**, 104–113, DOI: 10.1007/s11095-007-9350-0.
92 G. Li, A. Badkar, S. Nema, C. S. Kolli and A. K. Banga, *Int. J. Pharm.*, 2009, **368**, 109–115, DOI: 10.1016/j.ijpharm.2008.10.008.
93 T. Miyano, Y. Tobinaga, T. Kanno, Y. Matsuzaki, H. Takeda, M. Wakui and K. Hanada, *Biomed. Microdevices*, 2005, **7**, 185–188, DOI: 10.1007/s10544-005-3024-7.
94 R. F. Donnelly, D. I. Morrow, T. R. Singh, K. Migalska, P. A. McCarron, C. O'Mahony and A. D. Woolfson, *Drug Dev. Ind. Pharm.*, 2009, **35**, 1242–1254, DOI: 10.1080/03639040902882280.
95 C. J. Martin, C. J. Allender, K. R. Brain, A. Morrissey and J. C. Birchall, *J. Controlled Release*, 2012, **158**, 93–101, DOI: 10.1016/j.jconrel.2011.10.024.
96 H. J. Choi, B. J. Bondy, D. G. Yoo, R. W. Compans, S. M. Kang and M. R. Prausnitz, *J. Controlled Release*, 2013, **166**, 159–171, DOI: 10.1016/j.jconrel.2012.12.002.
97 Y.-C. Kim, F.-S. Quan, R. W. Compans, S.-M. Kang and M. R. Prausnitz, *Pharm. Res.*, 2010, **28**, 135–144, DOI: 10.1007/s11095-010-0134-6.
98 X. Hong, L. Wei, F. Wu, Z. Wu, L. Chen, Z. Liu and W. Yuan, *Drug Des., Dev. Ther.*, 2013, **7**, 945–952, DOI: 10.2147/DDDT.S44401.
99 Y. Q. Ye, J. C. Yu, D. Wen, A. R. Kahkoska and Z. Gu, *Adv. Drug Delivery Rev.*, 2018, **127**, 106–118, DOI: 10.1016/j.addr.2018.01.015.
100 J. W. Lee, M. R. Han and J. H. Park, *J. Drug Targeting*, 2013, **21**, 211–223, DOI: 10.3109/1061186x.2012.741136.
101 D. D. Zhu, Q. L. Wang, X. B. Liu and X. D. Guo, *Acta Biomater.*, 2016, **41**, 312–319, DOI: 10.1016/j.actbio.2016.06.005.
102 Z. M. Luo, W. J. Sun, J. Fang, K. Lee, S. Li, Z. Gu, M. R. Dokmeci and A. Khademhosseini, *Adv. Healthcare Mater.*, 2019, **8**, 1801054, DOI: 10.1002/adhm.201801054.
103 Q. L. Wang, D. D. Zhu, Y. Chen and X. D. Guo, *Mater. Sci. Eng., C*, 2016, **65**, 135–142, DOI: 10.1016/j.msec.2016.03.097.
104 C. P. P. Pere, S. N. Economidou, G. Lall, C. Ziraud, J. S. Boateng, B. D. Alexander, D. A. Lamprou and D. Douroumis, *Int. J. Pharm.*, 2018, **544**, 425–432, DOI: 10.1016/j.ijpharm.2018.03.031.
105 R. D. Koyani, *J. Drug Delivery Sci. Technol.*, 2020, **60**, 102071, DOI: 10.1016/j.jddst.2020.102071.
106 J. Mao, H. Wang, Y. Xie, Y. Fu, Y. Li, P. Liu, H. Du, J. Zhu, L. Dong, M. Hussain, Y. Li, L. Zhang, J. Zhu and J. Tao, *J. Mater. Chem. B*, 2020, **8**, 928–934, DOI: 10.1039/c9tb00912d.
107 G. Cole, A. A. Ali, C. M. McCrudden, J. W. McBride, J. McCaffrey, T. Robson, V. L. Kett, N. J. Dunne, R. F. Donnelly and H. O. McCarthy, *Eur. J. Pharm. Biopharm.*, 2018, **127**, 288–297, DOI: 10.1016/j.ejpb.2018.02.029.
108 B. Z. Chen, M. Ashfaq, X. P. Zhang, J. N. Zhang and X. D. Guo, *J. Drug Targeting*, 2018, **26**, 720–729, DOI: 10.1080/1061186X.2018.1424859.
109 Y. K. Demir, Z. Akan and O. Kerimoglu, *PLoS One*, 2013, **8**, e77289, DOI: 10.1371/journal.pone.0077289.
110 M. He, G. Yang, S. Zhang, X. Zhao and Y. Gao, *J. Pharm. Sci.*, 2018, **107**, 1037–1045, DOI: 10.1016/j.xphs.2017.11.013.
111 M. B. Requena, A. D. Permana, J. D. Vollet-Filho, P. Gonzalez-Vazquez, M. R. Garcia, C. M. Goncalves De Faria, S. Pratavieira, R. F. Donnelly and V. S. Bagnato, *J. Biophotonics*, 2021, **14**, e202000128, DOI: 10.1002/jbio.202000128.
112 Y. Pastor, E. Larraneta, A. Erhard, G. Quincooces, I. Penuelas, J. M. Irache, R. Donnelly and C. Gamazo, *Vaccines*, 2019, **7**, 159–174, DOI: 10.3390/vaccines7040159.
113 M. Zaric, O. Lyubomska, O. Touzelet, C. Poux, S. Al-Zahrani, F. Fay, L. Wallace, D. Terhorst, B. Malissen, S. Henri, U. F. Power, C. J. Scott, R. F. Donnelly and A. Kissenpfennig, *ACS Nano*, 2013, **7**, 2042–2055, DOI: 10.1021/nn304235j.
114 P. C. DeMuth, W. F. Garcia-Beltran, M. L. Ai-Ling, P. T. Hammond and D. J. Irvine, *Adv. Funct. Mater.*, 2013, **23**, 161–172, DOI: 10.1002/adfm.201201512.
115 J. W. Lee, J. H. Park and M. R. Prausnitz, *Biomaterials*, 2008, **29**, 2113–2124, DOI: 10.1016/j.biomaterials.2007.12.048.
116 K. Tsioris, W. K. Raja, E. M. Pritchard, B. Panilaitis, D. L. Kaplan and F. G. Omenetto, *Adv. Funct. Mater.*, 2012, **22**, 330–335, DOI: 10.1002/adfm.201102012.
117 L. K. Vora, A. J. Courtenay, I. A. Tekko, E. Larraneta and R. F. Donnelly, *Int. J. Biol. Macromol.*, 2020, **146**, 290–298, DOI: 10.1016/j.ijbiomac.2019.12.184.
118 Y. K. Demir, Z. Akan and O. Kerimoglu, *PLoS One*, 2013, **8**, e63819, DOI: 10.1371/journal.pone.0063819.
119 A. R. J. Hutton, M. T. C. McCrudden, E. Larraneta and R. F. Donnelly, *J. Mater. Chem. B*, 2020, **8**, 4202–4209, DOI: 10.1039/d0tb00021c.
120 C.-H. Chen, V. B.-H. Shyu and C.-T. Chen, *Materials*, 2018, **11**, 1625, DOI: 10.3390/ma11091625.
121 S. Naito, Y. Ito, T. Kiyohara, M. Kataoka, M. Ochiai and K. Takada, *Vaccine*, 2012, **30**, 1191–1197, DOI: 10.1016/j.vaccine.2011.11.111.
122 S. Wei, G. Quan, C. Lu, X. Pan and C. Wu, *Biomater. Sci.*, 2020, **8**, 5739–5750, DOI: 10.1039/d0bm00914h.
123 K. Yu, X. Yu, S. Cao, Y. Wang, Y. Zhai, F. Yang, X. Yang, Y. Lu, C. Wu and Y. Xu, *Acta Pharm. Sin. B*, 2021, **11**, 505–519, DOI: 10.1016/j.apsb.2020.08.008.
124 Y. Park and B. Kim, *Korean J. Chem. Eng.*, 2017, **34**, 133–138, DOI: 10.1007/s11814-016-0240-1.
125 X. Jin, D. D. Zhu, B. Z. Chen, M. Ashfaq and X. D. Guo, *Adv. Drug Delivery Rev.*, 2018, **127**, 119–137, DOI: 10.1016/j.addr.2018.03.011.

126 M. S. B. Husain, A. Gupta, B. Y. Alashwal and S. Sharma, *Energy Sources, Part A*, 2018, **40**, 2388–2393, DOI: 10.1080/15567036.2018.1495786.
127 E. M. Vicente-Perez, E. Larraneta, M. T. C. McCrudden, A. Kissenpfennig, S. Hegarty, H. O. McCarthy and R. F. Donnelly, *Eur. J. Pharm. Biopharm.*, 2017, **117**, 400–407, DOI: 10.1016/j.ejpb.2017.04.029.
128 X. P. Zhang, B. B. Wang, W. X. Li, W. M. Fei, Y. Cui and X. D. Guo, *Eur. J. Pharm. Biopharm.*, 2021, **160**, 1–8, DOI: 10.1016/j.ejpb.2021.01.005.
129 H. S. Jung, K. S. Kim, S. H. Yun and S. K. Hahn, *Nanomedicine*, 2014, **9**, 743–745, DOI: 10.2217/nnm.14.47.
130 M. C. S. Barcelos, K. A. C. Vespermann, F. M. Pelissari and G. Molina, *Crit. Rev. Food Sci. Nutr.*, 2020, **60**, 1475–1495, DOI: 10.1080/10408398.2019.1575791.
131 G. Kang, S. Kim, H. Yang, M. Jang, L. Chiang, J. H. Baek, J. H. Ryu, G. W. Choi and H. Jung, *J. Cosmet., Dermatol.*, 2019, **18**, 1083–1091, DOI: 10.1111/jocd.12807.
132 J.-H. Park, C. B. Kim, H.-J. Lee, J. Y. Roh, J. M. Lee, H. J. Kim and J.-H. Park, *Drug Delivery Transl. Res.*, 2020, **10**, 791–800, DOI: 10.1007/s13346-020-00710-x.
133 V. Zvezdin, L. Peno-Mazzarino, N. Radionov, T. Kasatkina and I. Kasatkin, *Int. J. Cosmet. Sci.*, 2020, **42**, 369–376, DOI: 10.1111/ics.12627.
134 W. S. Shim, Y. M. Hwang, S. G. Park, C. K. Lee and N. G. Kang, *Bull. Korean Chem. Soc.*, 2018, **39**, 789–793, DOI: 10.1002/bkcs.11476.
135 M. T. C. McCrudden, A. Z. Alkilani, C. M. McCrudden, E. McAlister, H. O. McCarthy, A. D. Woolfson and R. F. Donnelly, *J. Controlled Release*, 2014, **180**, 71–80, DOI: 10.1016/j.jconrel.2014.02.007.
136 M. J. Garland, E. Caffarel-Salvador, K. Migalska, A. D. Woolfson and R. F. Donnelly, *J. Controlled Release*, 2012, **159**, 52–59, DOI: 10.1016/j.jconrel.2012.01.003.
137 M. T. C. McCrudden, A. Z. Alkilani, A. J. Courtenay, C. M. McCrudden, B. McCloskey, C. Walker, N. Alshraiedeh, R. E. M. Lutton, B. F. Gilmore, A. D. Woolfson and R. F. Donnelly, *Drug Delivery Transl. Res.*, 2015, **5**, 3–14, DOI: 10.1007/s13346-014-0211-1.
138 A. I. Camacho, J. M. Irache, J. de Souza, S. Sanchez-Gomez and C. Gamazo, *Vaccine*, 2013, **31**, 3288–3294, DOI: 10.1016/j.vaccine.2013.05.020.
139 A. E. Thurber, F. G. Omenetto and D. L. Kaplan, *Biomaterials*, 2015, **71**, 145–157, DOI: 10.1016/j.biomaterials.2015.08.039.
140 L. Meinel, S. Hofmann, V. Karageorgiou, C. Kirker-Head, J. McCool, G. Gronowicz, L. Zichner, R. Langer, G. Vunjak-Novakovic and D. L. Kaplan, *Biomaterials*, 2005, **26**, 147–155, DOI: 10.1016/j.biomaterials.2004.02.047.
141 J. A. Stinson, W. K. Raja, S. Lee, H. B. Kim, I. Diwan, S. Tutunjian, B. Panilaitis, F. G. Omenetto, S. Tzipori and D. L. Kaplan, *ACS Biomater. Sci. Eng.*, 2017, **3**, 360–369, DOI: 10.1021/acsbiomaterials.6b00515.
142 M. Zhu, Y. Liu, F. Jiang, J. Cao, S. C. Kundu and S. Lu, *ACS Biomater. Sci. Eng.*, 2020, **6**, 3422–3429, DOI: 10.1021/acsbiomaterials.0c00273.
143 Y. Zhang, K. Brown, K. Siebenaler, A. Determan, D. Dohmeier and K. Hansen, *Pharm. Res.*, 2012, **29**, 170–177, DOI: 10.1007/s11095-011-0524-4.
144 C. Edens, M. L. Collins, J. Ayers, P. A. Rota and M. R. Prausnitz, *Vaccine*, 2013, **31**, 3403–3409, DOI: 10.1016/j.vaccine.2012.09.062.
145 J. Park and Y.-C. Kim, *Drug Delivery Transl. Res.*, 2021, **11**, 205–213, DOI: 10.1007/s13346-020-00781-w.
146 J. Monkare, M. Pontier, E. E. M. van Kampen, G. Du, M. Leone, S. Romeijn, M. R. Nejadnik, C. O'Mahony, B. Slutter, W. Jiskoot and J. A. Bouwstra, *Eur. J. Pharm. Biopharm.*, 2018, **129**, 111–121, DOI: 10.1016/j.ejpb.2018.05.031.
147 Y. Chen, B. Z. Chen, Q. L. Wang, X. Jin and X. D. Guo, *J. Controlled Release*, 2017, **265**, 14–21, DOI: 10.1016/j.jconrel.2017.03.383.
148 M. C. He, B. Z. Chen, M. Ashfaq and X. D. Guo, *Drug Delivery Transl. Res.*, 2018, **8**, 1034–1042, DOI: 10.1007/s13346-018-0547-z.
149 J. Zhang, Y. Wang, J. Y. Jin, S. Degan, R. P. Hall, R. D. Boehm, P. Jaipan and R. J. Narayan, *JOM*, 2016, **68**, 1128–1133, DOI: 10.1007/s11837-016-1841-1.
150 J. H. Park, M. G. Allen and M. R. Prausnitz, *Pharm. Res.*, 2006, **23**, 1008–1019, DOI: 10.1007/s11095-006-0028-9.
151 P. T. Ko, I. C. Lee, M. C. Chen and S. W. Tsai, *J. Taiwan Inst. Chem. Eng.*, 2015, **51**, 1–8, DOI: 10.1016/j.jtice.2015.01.003.
152 M. C. Chen, M. H. Ling, K. Y. Lai and E. Pramudityo, *Biomacromolecules*, 2012, **13**, 4022–4031, DOI: 10.1021/bm301293d.
153 J. H. Jin, V. Reese, R. Coler, D. Carter and M. Rolandi, *Adv. Healthcare Mater.*, 2014, **3**, 349–353, DOI: 10.1002/adhm.201300185.
154 D. A. Castilla-Casadiego, H. Carlton, D. Gonzalez-Nino, K. A. Miranda-Munoz, R. Daneshpour, D. Huitink, G. Prinz, J. Powell, L. Greenlee and J. Almodovar, *Mater. Sci. Eng., C*, 2021, **118**, 111544, DOI: 10.1016/j.msec.2020.111544.
155 K. S. Ogueri, T. Jafari, J. L. Escobar Ivirico and C. T. Laurencin, *Regener. Eng. Transl. Med.*, 2019, **5**, 128–154, DOI: 10.1007/s40883-018-0072-0.
156 K. Madhavan Nampoothiri, N. R. Nair and R. P. John, *Bioresour. Technol.*, 2010, **101**, 8493–8501, DOI: 10.1016/j.biortech.2010.05.092.
157 Y. Cao, G. Mitchell, A. Messina, L. Price, E. Thompson, A. Penington, W. Morrison, A. O'Connor, G. Stevens and J. Cooper-White, *Biomaterials*, 2006, **27**, 2854–2864, DOI: 10.1016/j.biomaterials.2005.12.015.
158 S. J. Schmidt, B. D. Holt, A. M. Arnold and S. A. Sydlik, *RSC Adv.*, 2020, **10**, 8548–8557, DOI: 10.1039/c9ra10646d.
159 Q. Y. Li, J. N. Zhang, B. Z. Chen, Q. L. Wang and X. D. Guo, *RSC Adv.*, 2017, **7**, 15408–15415, DOI: 10.1039/c6ra26759a.
160 W. Li, J. Tang, R. N. Terry, S. Li, A. Brunie, R. L. Callahan, R. K. Noel, C. A. Rodriguez, S. P. Schwendeman and M. R. Prausnitz, *Sci. Adv.*, 2019, **5**, eaaw8145, DOI: 10.1126/sciadv.aaw8145.
161 K. T. M. Tran, T. D. Gavitt, N. J. Farrell, E. J. Curry, A. B. Mara, A. Patel, L. Brown, S. Kilpatrick, R. Piotrowska,

N. Mishra, S. M. Szczepanek and T. D. Nguyen, *Nat. Biomed. Eng.*, 2020, 13, DOI: 10.1038/s41551-020-00650-4.
162 J. Eum, Y. Kim, D. J. Um, J. Shin, H. Yang and H. Jung, *Micromachines*, 2021, **12**, 167, DOI: 10.3390/mi12020167.
163 G. Song, G. Jiang, T. Liu, X. Zhang, Z. Zeng, R. Wang, P. Li and Y. Yang, *ACS Biomater. Sci. Eng.*, 2020, **6**, 4116–4125, DOI: 10.1021/acsbiomaterials.0c00793.
164 B. Z. Chen, M. Ashfaq, D. D. Zhu, X. P. Zhang and X. D. Guo, *Macromol. Rapid Commun.*, 2018, **39**, 1800075, DOI: 10.1002/marc.201800075.
165 W. Yu, G. Jiang, Y. Zhang, D. Liu, B. Xu and J. Zhou, *J. Mater. Chem. B*, 2017, **5**, 9507–9513, DOI: 10.1039/c7tb02236k.
166 X. Yi, C. Wang, X. Yu, W. Su and Z. Yuan, *J. Biomed. Mater. Res., Part B*, 2021, **109**, 911–920, DOI: 10.1002/jbm.b.34755.
167 Y. H. Chiu, M. C. Chen and S. W. Wan, *Biomacromolecules*, 2018, **19**, 2278–2285, DOI: 10.1021/acs.biomac.8b00441.
168 M. Y. Qu, H. J. Kim, X. W. Zhou, C. R. Wang, X. Jiang, J. X. Zhu, Y. M. Xue, P. Tebon, S. A. Sarabi, S. Ahadian, M. R. Dokmeci, S. S. Zhu, Z. Gu, W. J. Sun and A. Khademhosseini, *Nanoscale*, 2020, **12**, 16724–16729, DOI: 10.1039/d0nr02759f.
169 B. Z. Chen, L. Q. Zhang, Y. Y. Xia, X. P. Zhang and X. D. Guo, *Sci. Adv.*, 2020, **6**, 11, DOI: 10.1126/sciadv.aba7260.
170 S. Wang, M. Zhu, L. Zhao, D. Kuang, S. C. Kundu and S. Lu, *ACS Biomater. Sci. Eng.*, 2019, **5**, 1887–1894, DOI: 10.1021/acsbiomaterials.9b00229.
171 J. G. Turner, L. R. White, P. Estrela and H. S. Leese, *Macromol. Biosci.*, 2021, **21**, 2000307, DOI: 10.1002/mabi.202000307.
172 K. Ita, *Pharmaceutics*, 2015, **7**, 90–105, DOI: 10.3390/pharmaceutics7030090.
173 R. F. Donnelly, T. R. Singh, M. J. Garland, K. Migalska, R. Majithiya, C. M. McCrudden, P. L. Kole, T. M. Mahmood, H. O. McCarthy and A. D. Woolfson, *Adv. Funct. Mater.*, 2012, **22**, 4879–4890, DOI: 10.1002/adfm.201200864.
174 R. F. Donnelly, M. T. C. McCrudden, A. Z. Alkilani, E. Larraneta, E. McAlister, A. J. Courtenay, M. C. Kearney, T. R. R. Singh, H. O. McCarthy, V. L. Kett, E. Caffarel-Salvador, S. Al-Zahrani and A. D. Woolfson, *PLoS One*, 2014, **9**, e111547, DOI: 10.1371/journal.pone.0111547.
175 R. Al-Kasasbeh, A. J. Brady, A. J. Courtenay, E. Larraneta, M. T. C. McCrudden, D. O'Kane, S. Liggett and R. F. Donnelly, *Drug Delivery Transl. Res.*, 2020, **10**, 690–705, DOI: 10.1007/s13346-020-00727-2.
176 A. V. Romanyuk, V. N. Zvezdin, P. Samant, M. I. Grenader, M. Zemlyanova and M. R. Prausnitz, *Anal. Chem.*, 2014, **86**, 10520–10523, DOI: 10.1021/ac503823p.
177 H. Chang, M. J. Zheng, X. J. Yu, A. Than, R. Z. Seeni, R. J. Kang, J. Q. Tian, D. P. Khanh, L. B. Liu, P. Chen and C. J. Xu, *Adv. Mater.*, 2017, **29**, 1702243, DOI: 10.1002/adma.201702243.
178 M. Zheng, Z. Wang, H. Chang, L. Wang, S. W. T. Chew, D. C. S. Lio, M. Cui, L. Liu, B. C. K. Tee and C. Xu, *Adv. Healthcare Mater.*, 2020, **9**, 1901683, DOI: 10.1002/adhm.201901683.
179 S. X. Yang, F. Wu, J. G. Liu, G. R. Fan, W. Welsh, H. Zhu and T. Jin, *Adv. Funct. Mater.*, 2015, **25**, 4633–4641, DOI: 10.1002/adfm.201500554.
180 R. Y. He, Y. Niu, Z. D. Li, A. Y. Li, H. Yang, F. Xu and F. Li, *Adv. Healthcare Mater.*, 2020, **9**, 1901201, DOI: 10.1002/adhm.201901201.
181 E. Y. Jeon, J. Lee, B. J. Kim, K. I. Joo, K. H. Kim, G. Lim and H. J. Cha, *Biomaterials*, 2019, **222**, 119439, DOI: 10.1016/j.biomaterials.2019.119439.
182 S. Y. Yang, E. D. O'Cearbhaill, G. C. Sisk, K. M. Park, W. K. Cho, M. Villiger, B. E. Bouma, B. Pomahac and J. M. Karp, *Nat. Commun.*, 2013, **4**, 1702, DOI: 10.1038/ncomms2715.
183 J. G. Hardy, E. Larraneta, R. F. Donnelly, N. McGoldrick, K. Migalska, M. T. C. McCrudden, N. J. Irwin, L. Donnelly and C. P. McCoy, *Mol. Pharmaceutics*, 2016, **13**, 907–914, DOI: 10.1021/acs.molpharmaceut.5b00807.
184 V. Zvezdin, T. Kasatkina, I. Kasatkin, M. Gavrilova and O. Kazakova, *Int. J. Cosmet. Sci.*, 2020, **42**, 429–435, DOI: 10.1111/ics.12636.
185 E. P. Yalcintas, D. S. Ackerman, E. Korkmaz, C. A. Telmer, J. W. Jarvik, P. G. Campbell, M. P. Bruchez and O. B. Ozdoganlar, *Pharm. Res.*, 2020, **37**, 33, DOI: 10.1007/s11095-019-2748-7.
186 A. Ono, S. Ito, S. Sakagami, H. Asada, M. Saito, Y. S. Quan, F. Kamiyama, S. Hirobe and N. Okada, *Pharmaceutics*, 2017, **9**, 13, DOI: 10.3390/pharmaceutics9030027.
187 M. Younes, G. Aquilina, L. Castle, K. H. Engel, P. Fowler, P. Furst, R. Gurtler, U. Gundert-Remy, T. Husoy, M. Manco, W. Mennes, P. Moldeus, S. Passamonti, R. Shah, D. H. Waalkens-Berendsen, D. Wolfle, M. Wright, P. Boon, R. Crebelli, A. Di Domenico, M. Filipic, A. Mortensen, R. Woutersen, H. Van Loveren, A. Giarola, F. Lodi, A. M. Rincon, A. Tard, M. J. F. Fernandez and E. P. F. A. Flavour, *EFSA J.*, 2020, **18**, 43, DOI: 10.2903/j.efsa.2020.6215.
188 J. Arya, S. Henry, H. Kalluri, D. V. McAllister, W. P. Pewin and M. R. Prausnitz, *Biomaterials*, 2017, **128**, 1–7, DOI: 10.1016/j.biomaterials.2017.02.040.
189 B. Pamornpathomkul, T. Ngawhirunpat, I. A. Tekko, L. Vora, H. O. McCarthy and R. F. Donnelly, *Eur. J. Pharm. Sci.*, 2018, **121**, 200–209, DOI: 10.1016/j.ejps.2018.05.009.
190 T. Kean and M. Thanou, *Adv. Drug Delivery Rev.*, 2010, **62**, 3–11, DOI: 10.1016/j.addr.2009.09.004.
191 M. Azmana, S. Mahmood, A. R. Hilles, U. K. Mandal, K. A. S. Al-Japairai and S. Raman, *J. Drug Delivery Sci. Technol.*, 2020, **60**, 101877, DOI: 10.1016/j.jddst.2020.101877.
192 J. Halder, S. Gupta, R. Kumari, G. D. Gupta and V. K. Rai, *J. Pharm. Innovation*, 2020, 1–8, DOI: 10.1007/s12247-020-09460-2.
193 R. S. J. Ingrole, E. Azizoglu, M. Dul, J. C. Birchall, H. S. Gill and M. R. Prausnitz, *Biomaterials*, 2021, **267**, 120491, DOI: 10.1016/j.biomaterials.2020.120491.